Actin networks: assembly and force production

Julie Theriot

Polymerizing networks of actin filaments are capable of exerting significant mechanical forces used by eukaryotic cells and their prokaryotic pathogens to change shape or to move. In several biological systems where the energy derived from nonequilibrium actin polymerization is used to generate propulsive force, actin networks demonstrate the ability to perform large-scale self-organization to create a polarized array. We are dissecting the biochemical and biophysical basis of actin network self-organization in several model systems.

The simplest case where a dendritically branched actin filament network can be seen to generate spontaneous large-scale polarity is in the case of spherical polystyrene beads coated uniformly with a protein that catalyzes actin nucleation via the Arp2/3 complex, such as ActA from the intracellular bacterial pathogen Listeria monocytogenes (Fig. 1). Initially the spheres are surrounded by a uniform cloud of actin that can convert to a polarized, motile "comet tail" in a manner that is sensitive to properties of the particle surface including size and surface density of ActA (1).

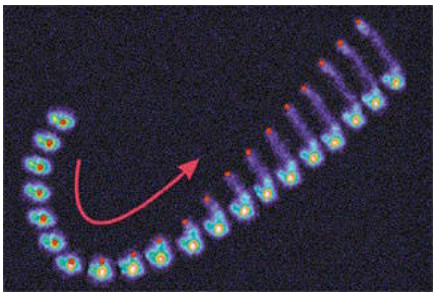

Fig. 1. Composite time series showing spontaneous symmetry-breaking of an actin cloud surrounding a spherical polystyrene bead coated uniformly with ActA. Bead position is shown in red. Actin filament density is shown in pseudocolor with cool colors representing low densities. Frames are separated by 10 sec.

ActA coating can confer motility on artificial particles other than polystyrene beads, including phospholipid vesicles (2, 3). Formation of actin comet tails on vesicle surfaces causes deformation of the vesicle shape. These deformations enable us to estimate the spatial distribution and magnitude of actin-dependent forces on the vesicle surface (Fig. 2). The inward compression force exerted by actin polymerization orthogonal to the direction of motion is >10-fold greater in magnitude than the component of the force exerted in the direction of motion. Furthermore, there is a spatial segregation of the pushing and retarding forces, such that pushing predominates along the sides of the vesicle, although retarding forces predominate at the rear. The dominance of compression forces and the functional separation between pushing and retarding forces are consistent with aspects of both mesoscopic and microscopic biophysical models for force generation in this system (4, 5).

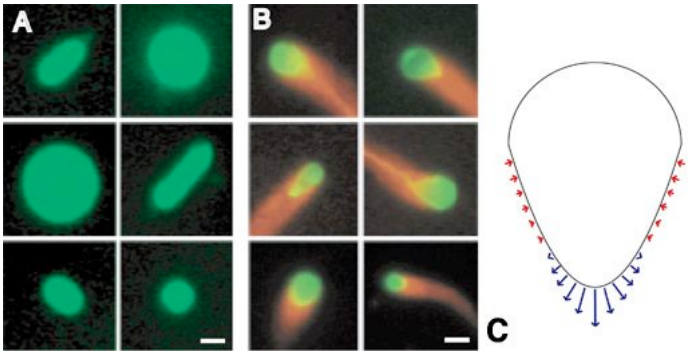

Fig. 2. Deformations of ActA-coated phospholipid vesicles due to actin comet tail formation. A. In the absence of ActA, vesicles assume spherical or prolate shapes. B. After comet tail formation, vesicles are distorted with the comet tail associated with the narrower end. C. Distribution of actin-dependent forces calculated on the vesicle surface (red net inward, blue net outward). From Ref. 2.

Actin-based motility of live L. monocytogenes is persistent and unidirectional, with the rod-shaped bacteria moving parallel to their long axis. In contrast to the simplified artificial particle systems, the bacteria have inherent structural polarity and express the ActA protein at a higher density on one pole. In order to determine whether the characteristic orientation of the bacteria is due to bacterial cell shape or polar expression of ActA, we have compared the motile behavior of spherical polystyrene beads uniformly coated with ActA to the behavior of polystyrene ellipsoidal beads. Ellipsoidal beads of two different aspect ratios were able to form comet tails and move in any orientation. Most beads formed tails either parallel to their long axis or perpendicular to their long axis, with a minority moving diagonally or switching orientations while moving. The average speed for all particles was identical regardless of shape or orientation. This indicates that the polarity of bacterial motility must be based primarily on the underlying polarity of the ActA protein and not on a physical preference for movement parallel to the long axis.

In the vesicle system describe above, the surface of the particle is fluid as well as deformable, and ActA can redistribute such that it is most highly concentrated at the rear of the vesicle, at the same location where retarding forces dominate (2, 3). In contrast, ActA is thought to be immobile on the surface of L. monocytogenes or polystyrene beads. To examine the contribution of surface fluidity to the establishment of movement polarity, we coated the surface of ellipsoidal beads with a fluid phospholipid bilayer prior to addition of ActA. Surprisingly, this treatment resulted in a new emergent phenotype not previously seen with any artificial particles: peristent circular movement (Fig. 3). We are currently investigating how the force balances at the particle surface may give rise to this unique steady state.

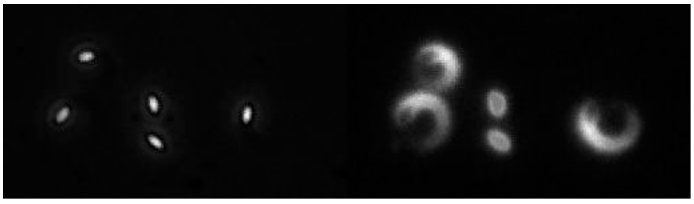

Fig. 3. Persistent circular movement by ellipsoidal beads coated with a phospholipid bilayer. Left, phase contrast image. Right, rhodamine-actin fluorescence. The two particles in the middle have not yet broken symmetry.

A similar dendritic actin meshwork is responsible for the extension of the lamellipodium at the leading edge of motile cells including fish epidermal keratocytes. At steady state, keratocyte movement is persistent and unidirectional and the cells maintain a simple, stereotyped, polar geometry. Maintenance of the motile steady state can be modeled based on assumptions of the balance of protrusion and contraction rates (6) or even with molecular detail (7). As with movement driven by comet tails, the constant polar moving state of keratocytes is preceded by a nonpolar, stationary state. We have developed a technique to isolate large numbers of stationary keratocytes. Stationary keratocytes have a circular morphology. Motile keratocytes have a half-moon shape with a large lamellipodia that carries the cell body on its dorsal surface and are capable of very rapid movement (up to 1 m/s). Over time, circular stationary keratocytes were observed to break symmetry spontaneously and generate a well-defined and persistent structural polarity in the absence of extrinsic spatial cues. We wished to determine whether spontaneous polarity was generated by specification of the leading edge (as in chemotaxis) or by specification of the trailing edge. Time-lapse phase contrast microscopy indicated that during spontaneous motility initiation the rear of the cell retracted first, followed by forward translocation of the cell body and finally the front cell margin, over a period of ~200-400 seconds (Fig. 4). This suggests that spontaneous motility initiation in keratocytes involves changes in the rear of the cell that are propagated to the leading edge, in contrast to the polarization of chemotactic cells in response to stimulation, where the leading edge is specified first.

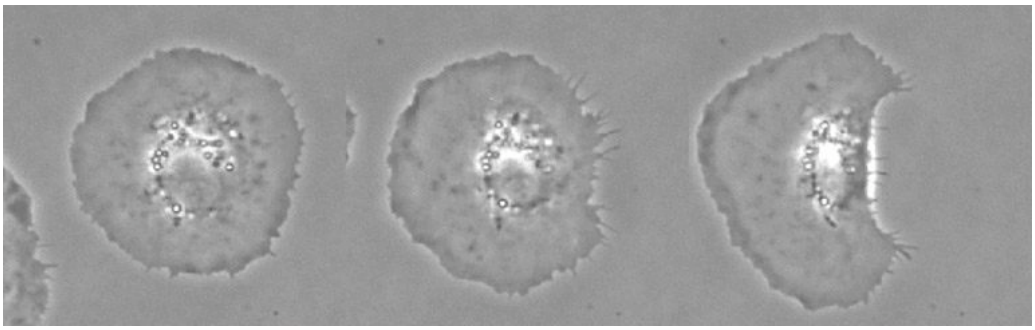

Fig. 4. Spontaneous symmetry-breaking and movement initiation in a fish keratocyte. Right, circular stationary cell. Middle, polarity initiation with retraction at the right. Left, fully polarized cell initiating movement. Frames are separated by about 2 min.

References:

1. Cameron LA, Footer MJ, van Oudenaarden A, Theriot JA. 1999. Motility of ActA protein-coated microspheres driven by actin polymerization. Proc Natl Acad Sci U S A. 96:4908-13.

2. Giardini PA, Fletcher DA, Theriot JA. 2003. Compression forces generated by actin comet tails on lipid vesicles. Proc Natl Acad Sci U S A. 100:6493-8.

3. Upadhyaya A, Chabot JR, Andreeva A, Samadani A, van Oudenaarden A. 2003. Probing polymerization forces by using actin-propelled lipid vesicles. Proc Natl Acad Sci U S A. 100:4521-6.

4. Gerbal F, Chaikin P, Rabin Y, Prost J. 2000. An elastic analysis of Listeria monocytogenes propulsion. Biophys J. 79:2259-75.

5. Mogilner A, Oster G. 2003. Force Generation by Actin Polymerization II: The Elastic Ratchet and Tethered Filaments. Biophys J. 84:1591-605.

6. Lee J, Ishihara A, Theriot JA, Jacobson K. 1993. Principles of locomotion for simple-shaped cells. Nature. 362:167-71.

7. Mogilner A, Edelstein-Keshet L. 2002. Regulation of actin dynamics in rapidly moving cells: a quantitative analysis. Biophys J. 83:1237-58.

Local dynamics and viscoelastic properties of cell biological systems

Denis Wirtz

How the cytoskeleton, a heterogeneous network of dynamic filamentous proteins, provides the cell with structural support is not well understood. Particle-tracking methods, which probe local mechanical properties, are well suited to test existing hypothesis derived from in vitro models of reconstituted cytoskeleton networks. My talk will present recent applications of single- and multiple-particle tracking microrheology to cell biological problems, with an emphasis on

networks of the semiflexible polymer F-actin. Extensive knowledge of the properties of these polymers allows a rigorous comparison between theory and experiments to a level rarely matched by synthetic polymers.

Introduction

Cell biology is entering a phase where biophysical methods hold center stage. In this postgenomic era, where genes and gene products of normal and pathological tissues are rapidly separated, identified and classified using high-throughput methods, there is a renewed emphasis on quantitative studies of cell behavior. This brief review focuses on some of the latest developments in colloidal science and polymer physics, which have led to new insight into cell mechanics and into the viscoelastic properties of the cytoskeletal filamentous proteins actin in vitro and in live cells.

Physical properties of F-actin networks

Filamentous actin (F-actin) is the polymer form of actin (G-actin; M = 43 kDa), which is expressed in all types of animal and human cells (Fig. 1). F-actin has attracted much attention from physicists, engineers, and biologists alike because of its fundamental role in key cellular functions, including cell migration, cytokinesis, endocytosis, cell adhesion, and because F-actin constitutes an extremely useful model for semiflexible polymers.

Semiflexible polymers constitute a vast and important class of polymers to which belong many molecules of technological and biological importance, including DNA and kevlar. F-actin is considered a semiflexible polymer because it has a mean contour length of L = 15 mm, which is similar to its mean persistence length, Lp = 17 mm. F-actin, a dynamic polymer of G-actin molecules, is uniquely versatile as its fundamental properties, including its mean length, length distribution, and bending rigidity, can readily be manipulated using actin-binding molecules. A key advantage of F-actin over synthetic polymers is that it can easily be visualized in the fluorescence microscope via specific labeling. Versatility and ease of visualization make F-actin an attractive polymer to test not only the predictions, but also the underlying molecular assumptions of dynamic theories of semiflexible polymers.

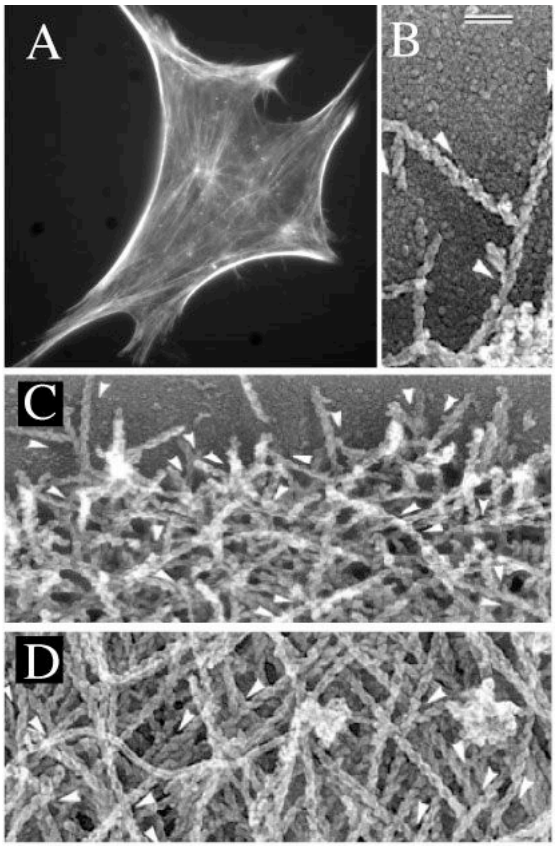

Fig. 1. F-actin organization in cells. a) F-actin organization in a Swiss 3T3 mouse fibroblast obtained by fixing and fluorescence-staining for F-actin. The low side of the figure is 120 mm. b) T junctions between actin filaments at the leading edge obtained by electron microscopy of detergent-extracted fish keratocyte. Bar is 0.1 mm and applies to figures b-d). c) F-actin organizartion is relatively homogenous structures at the leading edge of the cell, the cell side most proximal to the direction of migration. d) F-actin organization becomes more heterogeneous away from the leading edge. Directions of the slow growing ends of some filaments are shown by arrowheads located next to a filament. Figures b-d) are reproduced from the Journal of Cell Biology, 1997, vol 139, pp 397-515 by copyright permission of the Rockefeller University Press.

The rather extensive knowledge of the physical properties of F-actin (L, Lp, etc.) has allowed rigorous comparison between theory and experiments to a level rarely matched by synthetic polymers. Here, we briefly review the dynamical and rheological properties of Factin in dilute, semidilute, and concentrated solutions. In the dilute regime, Brownian dynamics simulations and theory predict that the stress relaxation modulus of semiflexible polymers scales as $G(t) \sim t^{-3/4}$ at short time scales. In an intermediate time-scale regime, $G(t) \sim t^{-5/4}$, a regime that is challenging to verify using conventional rheometers due to the small stresses generated in sheared solutions and the fragility of F-actin. Following the method of Dichtl and Sackmann, this intermediate behavior could be tested at a single-molecule level by tethering a small fluorescent particle to the polymer and tracking its Brownian motion with high temporal resolution using quadrant detection.

The onset of elasticity occurs at concentrations as low as ~0.1 mg/ml. Above this concentration, semidilute F-actin solutions have been shown (and used) to verify predictions of recent polymer-physics theories. These experimentally-verified predictions include the existence and concentration-dependence of a plateau modulus at low strain frequencies (Gp$\sim c^{7/5}$), the high-frequency-dependence of the elastic and loss moduli ($G'(\omega) \sim G''(\omega) \sim \omega^{3/4}$), the length-dependence of the relaxation time ($\tau_R \sim L^{3/2}$), and the concentration-dependence of the tube diameter inside which filaments are confined at short and intermediate time scales ($D \sim c^{-3/5}$). Analogous to the Doi-Edwards-de Gennes tube model, these results show that at time scales shorter than the time required for the lateral fluctuations of a test polymer to hit the tube walls formed by polymer entanglements, the dynamics of the test polymer is dominated by its high-frequency bending fluctuations, for which the relaxation modulus is $G(t) \sim t^{-3/4}$. At intermediate time scales, the test polymer becomes effectively confined by the tube and the relaxation modulus adopts a plateau value, $G(t) \sim G$p. Beyond the relaxation time, escape from the tube and terminal relaxation of the stress finally occur. Rheological methods show that, in the semidilute regime, F-actin solutions under stress display a slight strain-hardening, where the apparent modulus increases for increasing deformation amplitudes up to 3 - 7%, a behavior also observed in living cells. Past that threshold (i.e. yield strain), F-actin solutions soften rapidly. Theory predicts severe strain-softening at large strain amplitudes, but no strain-hardening at low strain amplitudes. This discrepancy between theory and experiment suggests the existence of (weak) interactions between F-actin polymers. A slightly higher-than-predicted value for the plateau modulus further supports the existence of non-steric interactions between filaments, may be due to electrostatic interactions.

Above a concentration of ~2 mg/ml, actin filaments form a liquid crystalline phase due to the local rigidity of F-actin. Concentrated solutions of F-actin display a low plateau modulus, Gp =30-50 dyn/cm^2, which is independent of concentration beyond ~2-3 mg/ml. In contrast, microrheological measurements reveal a mean modulus ~820 dyn/cm^2 in the actin-rich cortex of the cell, where actin concentration is ~100 mg/ml actin. Hence, solutions containing physiological concentrations of actin have a stiffness much lower than observed in living cells. Moreover, a cell exposed to highly specific actin-depolymerizing drugs softens dramatically, an effect accompanied by the rapid contraction of actin-rich cell extensions. F-actin's contribution to cell mechanical integrity is therefore essential but not sufficient.

Our knowledge about F-actin behavior in dilute, semidilute, and concentrated solutions sets the stage for the study of more complex, and indeed more physiological, structures where F-actin is crosslinked into stiffer architectures by crosslinking/bundling proteins. More than 60 actin-binding proteins have been identified in mammalian cells, among which seven are F-actin crosslinking/bundling proteins, proteins that mediate the formation of both orthogonal networks and ordered bundles. F-actin crosslinking/bundling proteins appear, sometimes concurrently, in specialized subcellular complexes, including lamellipodia, filopodia, stress fibers, and focal adhesions, which coordinate cell migration and cell spreading. The flexible

homodimeric actin-binding protein □-actinin stands out as an archetype of such actin crosslinking/bundling protein. F-actin/□-actinin solutions exhibit elastic moduli that nearly match those found in live cells. Because of its intrinsic flexibility, □-actinin crosslinks F-actin into orthogonal networks at low concentrations and into loose filament bundles at high concentrations. An increase in the temperature-modulated binding lifetime enhances both the plateau modulus and the hardening effect of F-actin networks under shear strains. However, the microheterogeneity of F-actin networks greatly increases for increasing □-actinin concentration. These two effects, variable binding lifetime and network microheterogeneity, are not explicitly incorporated in current models of F-actin networks.

Single- and multiple-particle tracking microrheology of gels, cells, and networks

The recent introduction of particle tracking microrheology (PTM) has opened a realm of possibilities in the characterization of novel materials and cell biological systems. Because it requires a small sample, PTM can readily be used for high-throughput screening of novel/expensive materials, such as specialty polymers, and biological specimen, such as lung mucus, synovial fluid, and blood. Unlike most rheometers, PTM can reliably probe low viscosity samples with exquisite sensitivity. Moreover, PTM provides quantitative information about the degree of heterogeneity of complex fluids.

PTM tracks the thermally-excited fluctuations of individual probe particles imbedded in a complex fluid to probe its local viscoelastic properties. The time-lag dependence mean squared displacement (MSD) of each particle, $\langle \Delta r^2(\tau) \rangle = \langle [x(t+\tau)-x(t)]^2+[y(t+\tau)-y(t)]^2 \rangle$, which is computed from the time-dependent coordinates of that particle, [x(t), y(t)], reveals the viscoelastic nature of the microenvironment in the immediate vicinity of each particle. If the MSD scales with time lag ($\langle \Delta r^2(\tau) \rangle \sim t$), then the microenvironment is liquidlike over seconds for laser-deflection tracking and < 1 min for video-tracking. In this case, the random viscous stresses created by the fluctuations of the particle are rapidly dissipated. If the MSD grows more slowly than time ($\langle \Delta r^2(\tau) \rangle \sim t^{\alpha}$ where $\alpha < 1$), the microenvironment is partially elastic. The random forces created by the fluctuating particle are met with restoring forces of equal or smaller magnitude. Faster-than-linear growth of the MSD signals either convection of the specimen or, more interestingly, directed transport via motor proteins, which actively move actin filaments in a network or bind organelles intracellularly. The MSD can either be transformed into a creep compliance trace, $J(\tau)=(\pi a/k_BT)\langle \Delta r^2(\tau) \rangle$ (*a* is the radius of the probe particle, T is the temperature of the specimen, and k_B is Boltzmann constant), or converted into frequency-dependent viscoelastic moduli via Laplace/Fourier transformation.

The motion of particles imbedded in a complex fluid or in a living cell can be monitored either by imaging or non-imaging methods. Laser deflection/quadrant detection is the (non-imaging) method used for the first proof of principle of PTM. The motion of a single particle deflects the incident beam of a low-power laser; the scattered light is collected by a quadrant photodiode detector, mounted onto a light microscope. Laser deflection/quadrant detection allows remarkable spatio-temporal resolution: ~1 nm displacements with 20 kHz time resolution are measured routinely. Therefore, local viscoelastic moduli spanning about 5 decades in frequencies are measured in seconds. This superior resolution has been exploited to probe the in-plane and out-of-plane shear elastic moduli of actin/vesicle complexes, actin dynamics in red blood cell's spectrin-actin network, and the local viscoelastic properties of an adherent cell by tracking the displacements of intracellular lipid-storage granules. These live-cell PTM measurements showed that the actin-rich cytoplasm exhibits elastic and loss moduli that scale as $G'(\omega) \sim G''(\omega) \sim \omega^{3/4}$, suggesting a viscoelastic character dominated by semiflexible polymers. PTM also demonstrated that subcellular regions of cytoplasm, the lamella and the perinuclear region, exhibit large difference in stiffness, a conclusion that could not have been reached

using traditional cell-mechanics methods, which are typically limited to global measurements of cell stiffness.

Laser deflection/quadrant detection has limitations as it allows tracking of only 1 or 2 particles at a time, which prevents real-time mapping of local viscoelastic properties. Moreover, only displacements smaller than ~0.3 mm can be monitored; hence particles imbedded in soft gels cannot be probed for a long time as their excursions step outside of detection. Multiple particle microrheology resolves many of these issues without much compromise in spatial resolution. The displacements of individual fluorescent or refractive particles are monitored simultaneously using either a CCD or SIT camera, typically at video rate (30 – 60 Hz). This imaging method retains a great spatial resolution of the displacements, ~5 nm, by tracking the centroid of the diffraction-limited image of each probe microsphere in the field of view. A key advantage of multiple particle tracking is that the shape of the distribution of the MSDs (or viscoelastic moduli) characterizes the degree of heterogeneity of the solution. For instance, the MSD

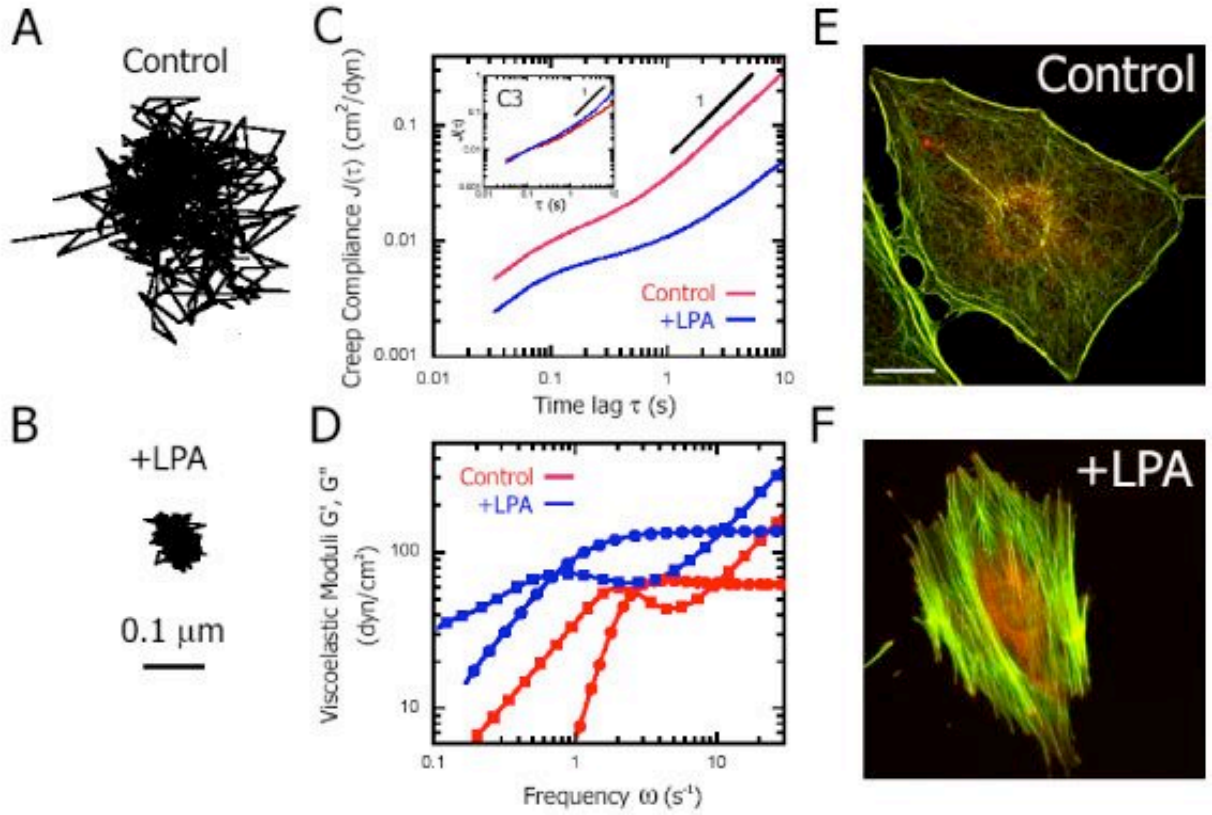

Figure 2. Cytomechanical response of Swiss 3T3 cells to Rho activation. A and B, Typical trajectories of nanospheres injected into the cytoplasm of serum-starved Swiss3T3 cells before (A) and 15 minutes after (B) treatment with 1 g/ml LPA. Scale bar indicates length scale for both trajectories. C, Ensemble-averaged creep compliance directly computed from the mean-squared displacements of the thermal motions of nanospheres injected into the cytoplasm of serum-starved Swiss 3T3 cells before (red) and 15 minutes after (blue) treatment with 1 g/ml LPA. (Inset), Ensemble-averaged creep compliance of the cytoplasm of serum-starved Swiss 3T3 cells injected with 10 g/ml C3, before (red) and after (blue) treatment with 1 g/ml LPA. D, Frequency-dependent viscous and elastic moduli, G"(£s) and G'(£s), obtained from ensemble-averaged creep compliances (C). G'(£s) is represented by circles and G"(£s) by squares. E and F, Fluorescent micrographs of serum-starved Swiss 3T3 cells before (E) and 15 minutes after (F) treatment with 1 g/ml LPA. Actin filaments (green) were visualized with Alexa 488 phalloidin, while focal adhesion complexes (red) were visualized with an antibody for vinculin and Alexa 566 goat anti-mouse. Scale bar represents 20 m.

distribution in homogenous solutions of polyethylene-oxyde or glycerol is symmetric and narrow; but becomes asymmetric and wide in F-actin networks and in cells. A practical method to analyze MSD distributions is to compare the skewness and kurtosis of the MSD distribution with those of the corresponding Gaussian distribution of same mean and standard deviation. An alternative method is to compute the contributions of the 10%, 25%, and 50% highest MSD values to the ensemble-averaged MSD, which are larger than 10%, 25%, and 50% for an inhomogenous solution. This type of analysis allows for the comparison of MSD distributions that encompass different MSD values as shown for F-actin and keratin.

Time-resolved multiple particle tracking, which monitors spatio-temporal variations of the microrheological properties in complex fluids, was recently used to uncover the underlying mechanism of F-actin gelation. A 1mg/ml actin solution forms an overlapping polymer network in ~ 1 min; yet the same solution takes ~ 1 h to reach a steady state elasticity. This slow gelation of F-actin is hypothesized to be due to the slow establishment of an homogeneous network. To test this model, time-resolved multiple particle tracking microrheology is introduced: the thermally-excited motion of hundreds of particles imbedded in an F-actin solution undergoing gelation is monitored in time and space. Time-resolved multiple particle-tracking shows that the degree of heterogeneity of an F-actin solution undergoing gelation decreased with time, tracking gelation kinetics. An increasing actin concentration increases the rate of actin polymerization, but decreases the rate of gelation and the rate of homogenization of F-actin solutions.

Another application of time-resolved multiple particle tracking microrheology consists in monitoring the spatio-temporal changes in cells subjected to pharmacological treatments or growth factors and LPA. Fig. 2 illustrates this application: serum-starved Swiss 3T3 fibroblasts are exposed to LPA, a small molecule that activates the small GTPase Rho and re-organizes the actin network.

One-point and two-point microrheology: the case of F-actin

Despite quantitative agreement between mechanical and particle tracking measurements for many colloidal and polymer solution systems, questions remain regarding the analysis of PTM experiments. The thermally excited motion of a probe particle imbedded in a biopolymer network may create a depletion zone, which could artificially decrease the apparent stiffness of the network. Moreover, the surface chemistry of the probe particle can affect the measurement of the mechanical properties of the network. Finally, local micro-heterogeneity of the network may greatly influence the estimation of the overall elasticity. These issues need to be addressed to refine current livecell particle-tracking micro-rheometers. Two-point microrheology suggests that the measurement of the pair-correlation of displacements could yield micro-mechanical parameters that are independent of the surface chemistry and size of the probe particles. One-point and two-point microrheology analysis of particle displacements yield different mechanical properties in F-actin. For a 1mg/ml F-actin solution, two-point correlation analysis yields elastic and viscous moduli that are very similar, $G' \approx G'' \approx 2$ dyn/cm^2 at 1 rad/s, which corresponds to a phase shift of 45°. Moreover, $G' \approx G'' \sim \omega^{1/2}$, which would imply that, at short time scales, F-actin resembles the stress relaxation dynamics of a flexible polymer. In startling contrast, one-point microrheology analysis shows a distinct plateau modulus at low frequencies (≈2-10 dyne/cm^2), a phase shift of $\delta \approx 25°$, i.e. an F-actin network behaves like a viscoelastic solid, and $G' \sim G'' \sim \omega^{3/4}$ at high frequencies, in agreement with magnetic-bead rheometry measurements. This suggests that methods involving forced bead movement and one-point microrheology measure an aspect of F-actin dynamic response which is different from, potentially complementary to, that measured by two-point microrheology.

Conclusions

Cytoskeleton microrheology is in its infancy, but particle-tracking methods are particularly well-suited to fill the gap between in vitro and in vivo systems. Many advances need to take place in theory, experimental methods, and choice of systems. A first step in that direction is to reconstitute more physiologically-relevant architectures, such as the dendritic actin structures mediated by the actin-binding protein Arp2/3 observed at the leading edge of a cell (Fig. 1b). Another is to investigate the synergistic potential of cytoskeletal polymers and crosslinking proteins (Fig. 1). Thoretical models of cytoskeleton micromechanics need to incorporate the finite lifetime of binding and the intrinsic flexibility of crosslinkers, nonsteric interfilament interactions, as well as network microheterogeneity. New optical tools need to be developed, which would combine the exquisite temporal resolution of laserdeflection and the superior statistics offered by video multiple-particle tracking.

Microtubule plus-ends: dynamics and interactions

Holly Goodson

The process of cell organization underlies fundamental biological processes ranging from polarized growth to multicellular development. Because many aspects of cell organization depend on the microtubule cytoskeleton, a major part of this initally diffuse problem can be reduced to two more tracktable questions: a) How is the microtubule cytoskeleton itself morphologically defined? b) How do other cellular components interact with microtubules? To answer these questions requires knowledge of the proteins that control microtubule (MT) dynamics and mediate cargo-MT interactions. Work in our laboratory is focused on a protein involved in the answers to both of these questions, CLIP-170.

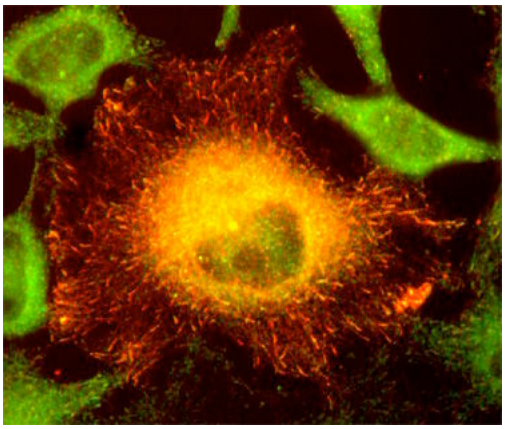

Figure 1. Localization of transfected CLIP-170 in red; endogenous p150 (a related plus-end tracking protein) is in green. (MeOH-fixed HeLa cells)

CLIP-170 is the founding member of a class of proteins with the surprising ability to dynamically track growing MT plus ends (Figure 1). Because of this unusual localization and the understanding that the tubulin conformation at the MT plus-end defines the propensity of the microtubule to grow or shrink (Figure 2), these "microtubule-plus-end tracking proteins" are predicted to regulate microtubule dynamics. Increasing evidence from a variety of sources indicates that they are also involved in mediation of interactions between "the rest of the cell" (membranes, chromosomes, the cell cortex) and microtubules.

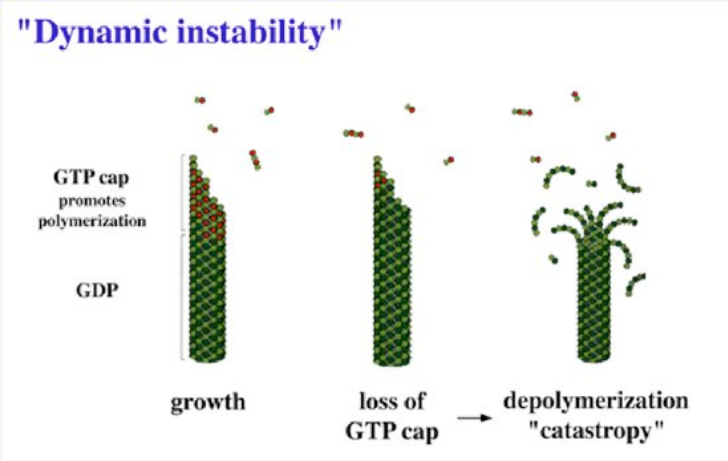

Figure 2. Mechanism of dynamic instability

To begin to address the role of CLIP-170 in these processes, it is necessary to better define its interactions with microtubules. In particular, we are investigating the mechanism of its plus-end tracking activity and its effect of microtubule dynamics. Our experiments indicate that CLIP-170 tracks MT plus ends by first associating with unpolymerized tubulin, then copolymerizing, then falling off of older areas of the polymer, most likely by a mechanism involving CLIP-170 phosphorylation (Figure 3). Our experiments show that CLIP-170 has very high affinity (~30nM) for unpolymerized tubulin and indicate that CLIP-170 is more of a tubulin binding protein than a microtubule binding protein. Though models where CLIP-170 would track MT plus ends by recognizing some plus-end specific conformation (the GTP cap) are attractive, the sum of our data argue against these models. We propose that the preassociation/ copolymerization model is a plausible mechanism by which the large number of unrelated plus-end tracking proteins could accomplish the same remarkable behavior.

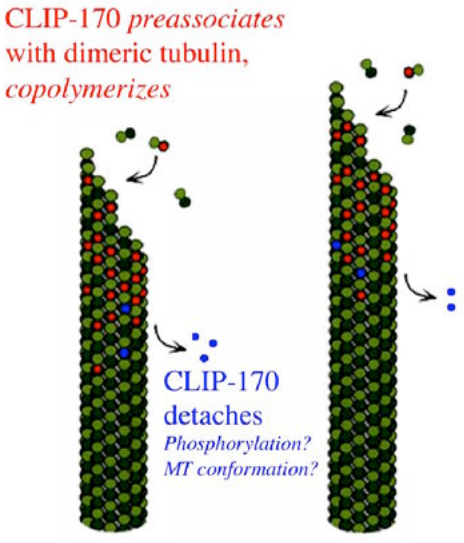

*Figure 3. Working model of CLIP-170 plus-end tracking behavior. Note that speckle analysis demonstrates that CLIP-170 does **not** move on the microtubule.*

In vitro dynamic instability assays show that CLIP-170 does indeed alter dynamics of pure tubulin in vitro, suppressing catastrophe and enhancing rescue. These observations are

consistent with reported effects of interfering with CLIP-170 function in vivo, and are the first demonstration of a direct effect of a plus end tracking protein on microtubule dynamics.

The idea that membranes can be organized by microtubules is well-established. The observation that CLIP-170 alters microtubule dynamics and is also involved in membrane-microtubule interactions leads to the idea that it may be involved in a system of "organizational feedback", allowing membranous cargo or other subcellular constituents to influence microtubule morphology. Consistent with this idea, plus-end tracking proteins appear to be involved in communication between microtubules and the cell cortex resulting in microtubule capture/selective stabilization. As originally postulated by Mitchison and Kirschner, selective stabilization could be a powerful force for cell polarization and morphological change (Figure 4). There is also evidence that CLIP-170 is involved in global regulation of microtubule dynamics. In summary, microtubule plus-end tracking proteins are physically and biochemically positioned to be a key part of these fundamental organizational processes.

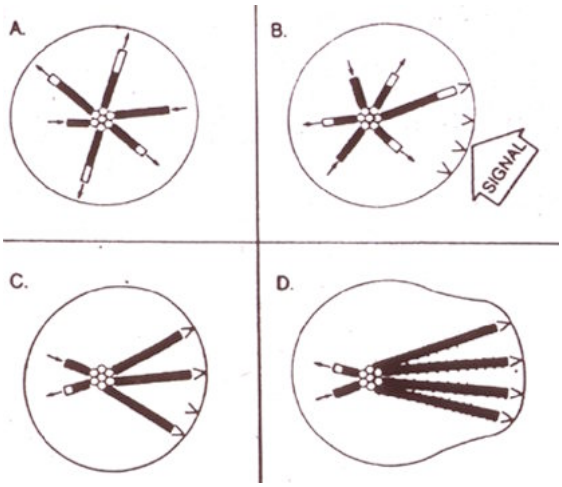

Figure 4. Selective stabilization and morphological change; from Cell 45:329 1986

Spindle pole assembly and function

Duane Compton

The spindle is a complex microtubule-based structure responsible for chromosome movement and segregation (Figure 1). Minus ends of spindle microtubules are focused at spindle poles which are the sites of chromatid convergence upon anaphase onset. In many cell types centrosomes are located at spindle poles as a consequence of their role in microtubule nucleation. However, centrosomes are not necessary for spindle pole organization or function, as demonstrated by the lack of centrosomes in some cell types and experiments where centrosomes have been eliminated from cells. Instead, microtubule minus-ends are focused at spindle poles by non-centrosomal proteins, including the structural protein NuMA and microtubule motor proteins dynein (with its activating complex dynactin), HSET and Eg5. These proteins work in concert to focus microtubule minus-ends and tether centrosomes to the spindle pole through microtubule crosslinking and/or motor activity.

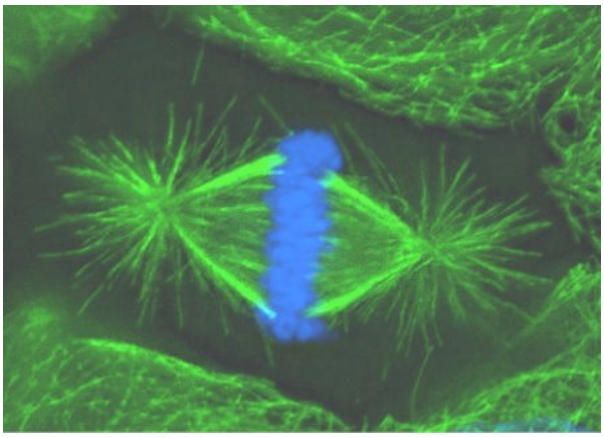

Figure 1. During metaphase of mitosis chromosomes (blue) align at the spindle equator. Minus ends of microtubules (green) within the spindle are focused at two spindle poles.

To investigate mechanisms of microtubule focusing at spindle poles we utilize a combined approach that involves in vitro biochemistry, in vivo cell biology, and computer modeling. In a cell free system microtubules are organized into asters (Figure 2) by the structural protein NuMA and motor proteins dynein (with its activating complex dynactin), HSET and Eg5. Extensive biochemical characterization of these microtubule asters indicates that the five non-centrosomal proteins mentioned above are the only proteins responsible for microtubule aster organization (Mack et al., 2001). Experiments where each protein has been inhibited alone or in various combinations has revealed important relationships between these proteins. For example, the minus end-directed motor activity of either dynein or HSET is sufficient for microtubule organization. Also, there is antagonism between motors of opposite polarity (Mountain et al., 1999).

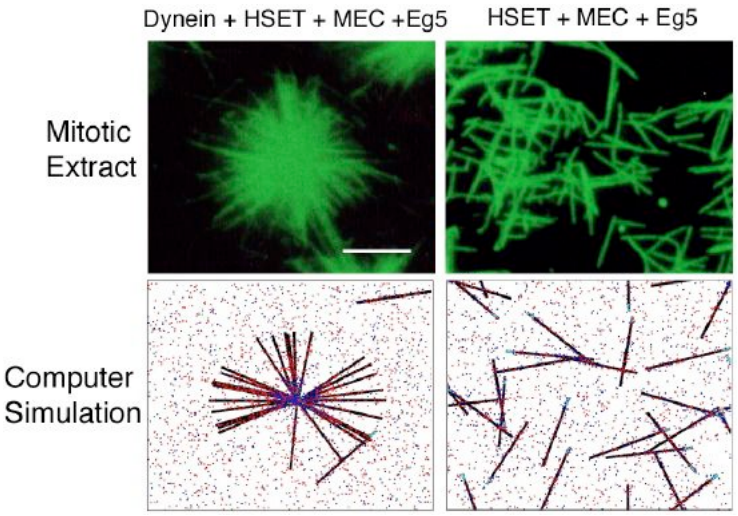

Figure 2. Microtubules in a mitotic extract form asters in the presence of dynein, HSET, NuMA (MEC), and Eg5 activities, but are randomly arranged if dynein is depleted. Computer simulation of these proteins yields similar results to the mitotic extract.

To understand how each protein contributes to microtubule organization and the nature of the relationships among these proteins we have utilized computer simulation (Figure 2). Computer simulation allows very fine-grained control of the microtubule motor and crosslinking activities. That work has led to a mechanistic model that states that the combination of two aggregate properties, Net Minus end-directed Force and microtubule Crosslinking Orientation Bias, determine microtubule organization. This model utilizes motor and non-motor proteins, accounts for motor antagonism, and predicts that alterations in crosslinking orientation bias should compensate for deficits in motor activity. We tested that prediction in the mammalian

mitotic extract and, consistent with the model, found that increasing the contribution of microtubule crosslinking by NuMA compensated for the loss of Eg5 motor activity. Thus, this model proposes a precise mechanism of action of each non-centrosomal protein during microtubule aster organization, and suggests that microtubule organization in spindles involves both motile forces from motors and static forces from non-motor crosslinking proteins.

References:

V. Mountain et al. (1999) J. Cell Biol. 147:351-365

G.J. Mack & D.A. Compton (2001) Proc. Nat. Acad. Sci. 98:14434-14439

Computer simulations of cytoskeletal dynamics

Jonathan Alberts and Garrett Odell

Lifelike behavior of a cell arises from interactions among huge numbers of molecules spun from the cell's genes - interactions buffeted by, or brought about by, thermal agitation. How can we get a handle on the cell-level dynamics that emerge from such myriad molecular interactions? We think the best way to understand the molecular genesis of complex cellular behavior is to build detailed computational models that explicitly simulate a large number of biochemical and mechanical interactions among cytoskeletal parts.

Small-scale biological details, which we encode into simple interaction rules, can lead to complex emergent behavior in non-obvious ways. One of our goal is to uncover the dependence of this behavior on molecular interaction details. The behaviors we seek to model in this way are, we believe, 'computationally irreducible'. This means that there isn't a shortcut (i.e. a derivable set of old-fashioned field or continuum equations) that can predict the outcome; we must run ensembles of computer simulations to discover what happens. Our explorations of parametric dependence, and the consequences of changing ratios of different kinds of molecular parts, thus require substantial computational resources; currently, we employ an 80-cpu cluster of computers.

A choice of scale is required in any such model. In other words, we can't really build a single sufficiently detailed model that is useful in simulating any cellular process at any length scale. If we are interested in cell motility should we concern ourselves with the detailed motion and conformation of each individual molecule? When two proteins bind must we calculate the steric transformations by modeling interatomic forces and integrating with femto-second time-steps? Given current computational resources, we forego the world of molecular dynamics and model from a molecular mechanics perspective. Here we represent protein assemblies by their bulk properties. For example, an actin filament is a homogeneous, isotropic, and flexible rod characterized by its length, cross-section, and modulus of elasticity. Actin monomers can attach to (detach from) its ends, but we do not model it as a collection of interacting actin monomers.

At present our most mature computational model addresses bacterial motility. The motility of the Listeria monocytogenes is a popular model system for studying actin network dynamics; we

are extending that study with a detailed computational model of the sort described above (see Figure 1). We have also created our own suite of analysis/plotting tools to characterize salient features of bacterial motion – both real and simulated – in order to compare the two.

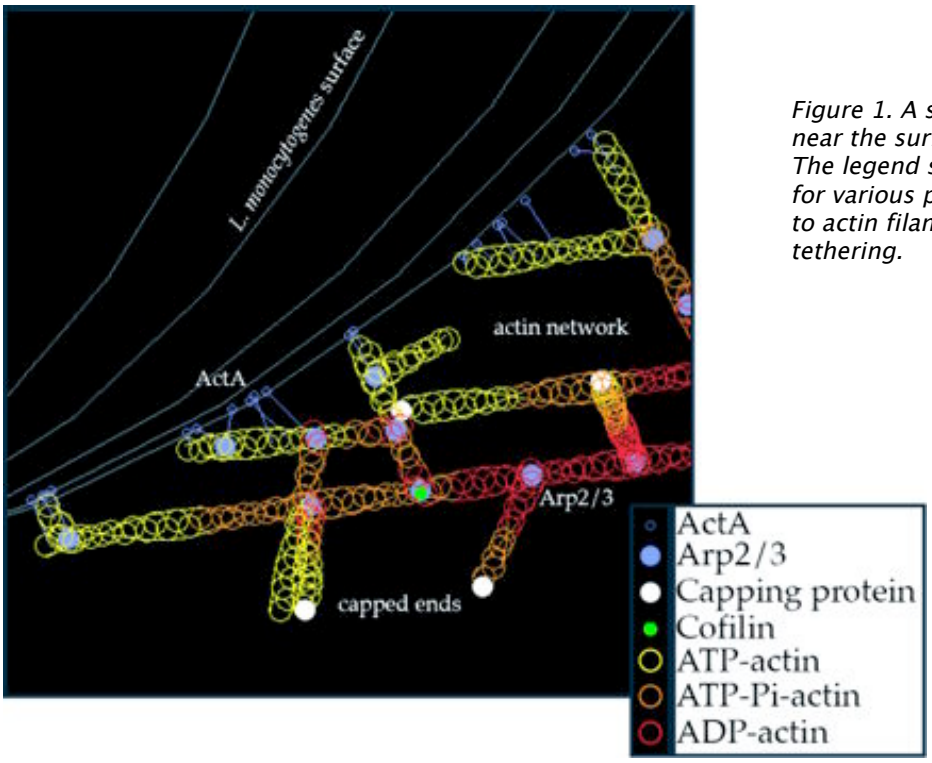

Figure 1. A snapshot of the action near the surface of the bacterium. The legend shows the color code for various players. Lines from ActA to actin filaments indicate transient tethering.

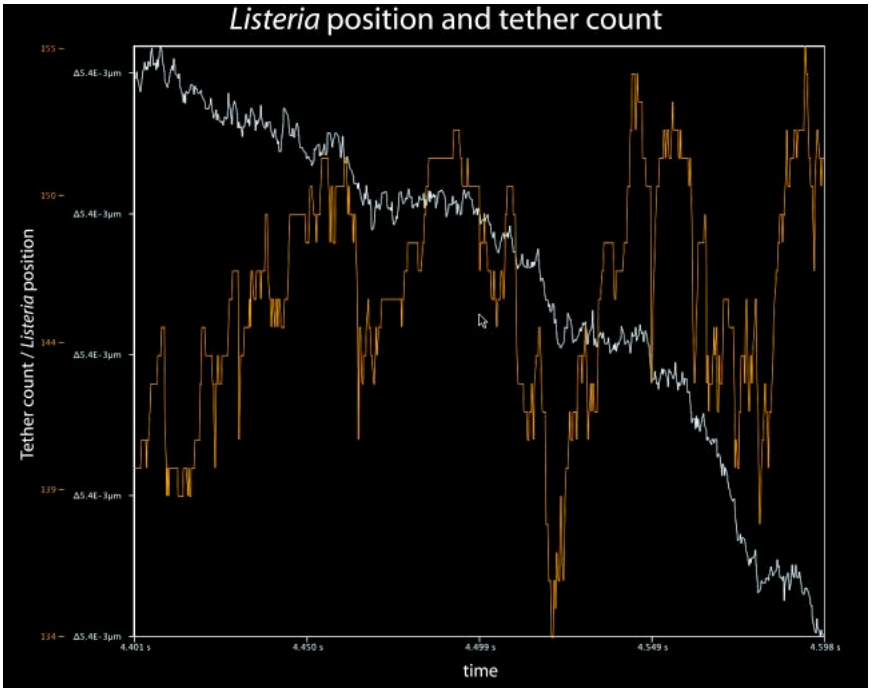

Figure 2. Simulation output showing bacterial position and the number of tethers between ActA proteins and actin filaments. This segment of the simulation demonstrates the saltatory step-like progress of the bacterium.

The literature on actin networks and Listeria motility provides a solid experimental base on which to build a realistic simulation. Most key rate constants governing actin network dynamics have been measured (see review Pollard et al 2000). Other work critical to our endeavor includes the identification of the sufficient and necessary proteins for reconstituted motion (Loisel et al, 1999), other biophysical treatments of actin network dynamics (Peskin et al, 1993; Mogilner & Oster, 1996; Mogilner & Oster 2003; Gerbal et al, 2000), and an earlier computational model of actin growth (Carlsson, 2001). Specifically relevant to the work we present in this workshop are biophysical experiments that have revealed discrete step-like motion on the nanometer scale (Kuo & McGrath, 2000; McGrath et al 2003).

Analysis of many simulations with a wide range of key parameter values demonstrates that the observed multi-phasic motion of Listeria, involving discrete steps, pauses, and continuous runs, emerges from cooperative binding and breaking of bonds between actin filaments and the bacteria. Figure 2 shows bacterial position data over a short period of one simulation in which step-like motion emerged. We find it encouraging that such small-scale and unexpected motility details are captured in our simulation.

We are currently developing simulation software, generalizing the Listeria actin polymerization ram, that will allow biologists interactively to specify the mechanical and biochemical interaction properties of numerous cytoskeletal parts such as various filaments such as actin and microtubules, various cross-linkers of these filaments, various motors such as kinesins, dyneins, cytoplasmic myosins, organelles such as nuclei, centrosomes, etc. Our software will constitute the mechanical properties of each small patch of the cortex/plasma membrane bounding a cell from the nearby population of relevant cytoskeletal parts. Simulated cells will

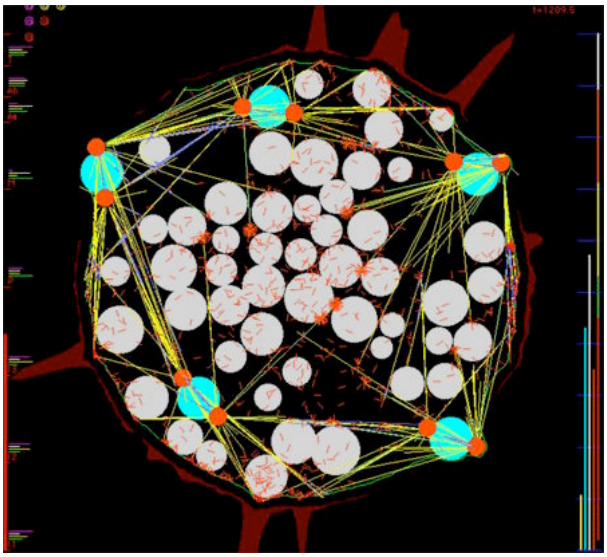

Figure 3. Frame from a movie simulating in 2-D the microtubule-driven migration of nuclei in a syncytial fruit fly embryo, the eruption of cytoplasmic buds as nuclei first reach the cortex, the compaction of yolk particles into the embryo's interior, and the redistribution of filamentous actin in the embryo's cortex.

contain whatever numbers of the various parts that the user specifies. Our computer programs will then generate the viscous-dominated Newtonian force and torque balance equations for each of the very many cytoskeletal parts and solve them numerically to determine the trajectory through three-dimensional space each part will follow. We simulate the thermal agitation forces that cause Brownian motion. This will provide a computational tool that will allow us and others to perform *in silico* reconstitution experiments to explore what macroscale behavior might emerge from various ensembles of molecular parts given hypotheses on the pairwise interactions among them. We have preliminary code working well and we are confident that we have solved the difficult computational challenge of detecting every collision between all the parts, each of which is free to move to any location in response to forces that impinge on it. We have implemented a novel scheme to cope with the "infinite stiffness" of our system of ordinary

differential equations - stiffness that arises due to sudden collisions between parts. We will show computer-animated movies, typical frames from which appear below, that exhibit the apparently purposeful behavior that emerges from the simple interaction rules we hypothesize.

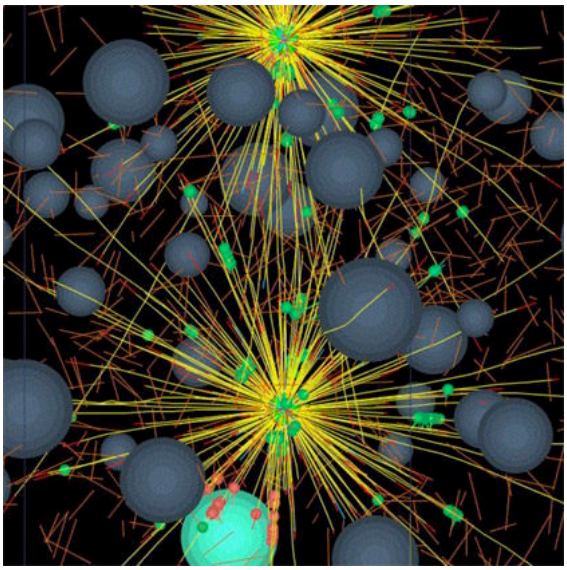

Figure 4. Frame from a proof-of-concept 3-D simulation of a small number of cytoskeletal parts moving each other around. It's Pinocchio just starting to twitch.

There is a profound difference between two-dimensional and three-dimensional models which we will discuss. Preliminary runs of our nascent three-dimensional model, in which we represent only about ten thousand parts, take about 16 hours to run on our fastest dual-processor 2.8Ghz Xeon computer. This extrapolates to an expectation that future realistic runs that involve up to millions of parts would require computer runs that would last many months on single computers. We are therefore developing software to distribute such huge calculations among hundreds of networked processors. These nuts and bolts computer science challenges (which real cells simply ignore as they use their myriad molecules to perform vast computations asynchronously in parallel) are important because the degree to which we succeed in solving them determines how realistic our simulations can be. We will use a significant part of our time to elicit audience opinions about the computational tricks we propose to implement to model the staggering complexity of cytoskeletal dynamics. We seek to learn which of these tricks arouse so much skepticism among biologists that we had best not use them.

Microtubule arrays

Vladimir Rodionov

Polarized radial arrays of cytoplasmic microtubules (MTs) with minus ends clustered at the cell center define the organization of the cytoplasm through interaction with molecular motors bound to the membrane organelles or chromosomes. MTs in the array serve as 'rails' for motor-mediated transport between membrane compartments and as a structural basis for organelle positioning in the cytoplasm. Formation of the radial MT array is generally assumed to be a result of nucleation at the centrosome, which often occupies position at the center of a cell. Recent studies indicate, however, that cells have a remarkable self-organizing capacity, that they can organize a radial array of MTs in the absence of the centrosome and that mechanisms

exist that position a focal point of converging MTs in the center of a cell. Here we examine the mechanisms of self-organization and self-centering of a radial MT array.

The self-organization mechanism.

To understand how MTs self-organize into a radial array we use cytoplasmic fragments of melanophores as an experimental system. In melanophores, thousands of pigment granules rapidly aggregate to the center or redisperse uniformly throughout the cytoplasm. The granules move by means of the minus-end-directed MT motor cytoplasmic dynein (aggregation) or a plus-end-directed motor of the kinesin family (dispersion). Microsurgically produced cytoplasmic fragments of melanophores lacking the centrosome rapidly form a polarized radial array after the stimulation of minus-end directed movement with adrenaline and position the pigment aggregate at the focal point of the converging MTs (Fig. 1).

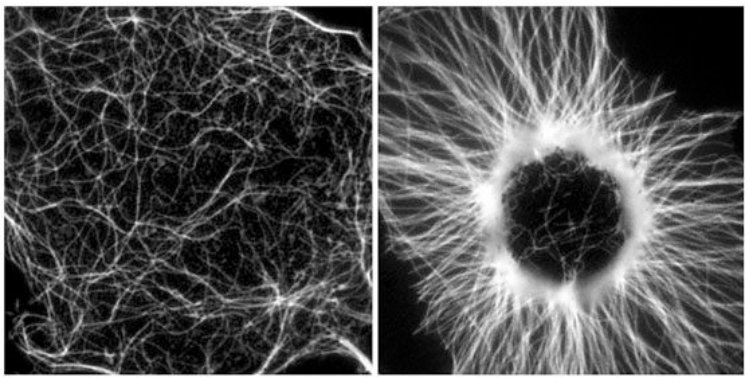

Figure 1. Live fluoresecence images of MTs in melanophore fragment before (left) and after (right) stimulation with adrenalin of dynein motors bound to pigment granules. Random MTs organize into a regular radial array.

We demonstrate that organization of MTs into a polarized radial array involves their continuous disassembly and reassembly. Growth of MTs is initiated on pigment granules that provide nucleation templates, but unlike the centrosome do not anchor the minus ends tightly. Frequent release and depolymerization from minus ends allows for rapid reorganization of a MT array. The spatial distribution of MTs at any given moment of time is determined by the location of pigment granules. However, pigment granules themselves do not remain stationary but are rapidly transported to the MT minus ends. Nucleation and frequent release of MTs superimposed on minus-end directed transport of the granule-associated nucleation sites eventually result in the formation of a radial array. We find that nucleation of MTs on pigment granules in the fragments is inhibited by dynein inhibitors. Further, we show that purified cytoplasmic dynein nucleates MTs in vitro. We conclude that self-organization mechanism involves MT dynamics and the activity of cytoplasmic dynein, which plays a dual role by participating in MT nucleation and by supporting minus-end directed transport of nucleation sites.

The nature of the centering force

It is known that centrosome positioning requires a radial array of cytoplasmic MTs that can exert pushing or pulling forces involving MT dynamics and the activity of cortical MT motors. It has also been suggested that actomyosin can play a direct or indirect role in this process.

To examine the centering mechanism, we disrupted MTs in BS-C-1 cells by local application of nocodazole, an inhibitor of MT assembly. Such local drug application induced disruption of MTs on the cell edge proximal, but not distal to the application site, thus introducing an imbalance in the MT-related forces applied to the centrosome. Local MT disruption induced rapid movement of the centrosome towards the micropipette in all examined cells. Remarkably, the

direction of the movement reversed if cells were pre-treated with inhibitors of actin and myosin contractility, - Rho inhibitor C3-transferase or MLCK inhibitor ML7, indicating that the centrosome positioning is controlled not only by MT, but by actin-dependent forces as well (Fig. 2). The change of the direction of the centrosome displacement in the presence of actomyosin inhibitors further suggests that the MT-dependent force involved in the centering is of pulling rather than pushing nature and that it acts in opposition to the actin-dependent forces. Such MT pulling could be produced by cortical cytoplasmic dynein. Indeed, in cells injected with dynein blocking antibody the centrosome failed to maintain its central position and was misplaced toward the nearest cell margin. Therefore a MT-dependent dynein pulling force plays a key role in the positioning of the centrosome at the cell center, and other forces applied to the centrosomal MTs, including actomyosin contractility, can contribute to this process.

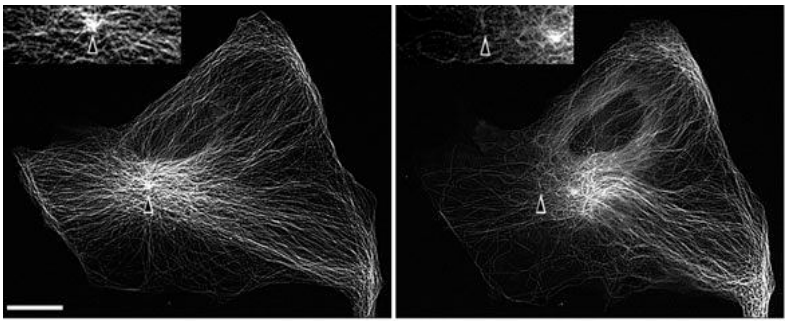

Fig. 2. Fluorescence images of the centrosome in the cell with inhibited RhoA activity before (left) and after (right) local application of nocodazole. Nocodazole was applied to the left margin. The initial position of the centrosome is indicated by black arrows. The centrosome moves away from the site of nocodazole application.

In conclusion, our results indicate that the MT dynamics and the activity of minus-end directed MT motors are essential for the self-organization and self-centering of a radial MT array. This cytomechanical module requires a surprisingly small number of functional components because cytoplasmic dynein plays multiple important roles in organization and positioning of the MT asters.

References:

1. Vorobjev, I.M., V.P.Malikov, and V.I.Rodionov. 2001. Self-organization of a radial microtubule array by dynein-dependent nucleation of microtubules. Proc. Natl. Acad. Sci. USA 98:10160-10165.

2. Burakon, A., E.Nadezhdina, B.Slepchenko, and V.Rodionov. 2003. Centrosome positioning in interphase cells. J. Cell Biol. (in press).

Mechanics of cell protrusions

Alex Mogilner

Fascinating phenomenon of cell crawling is based on a complex self-organized mechanochemical machine. Migrating cells are polarized, with the cell body at the rear, and a pseudopod - cytoskeletal protrusion largely devoid of organelles - at the front. The dynamic

cytoskeletal meshwork of the pseudopod is the basic engine pulling the crawling cell forward [5]. Pseudopodia of many motile cells, such as neutrophils, for example, are characterized by complex shapes and movements, which makes these cells' behavior hard to analyze. On the other hand, some cells possess relatively simple motile appendages and are more suitable to study the motile behavior. For example, fish epidermal keratocytes move steadily and rapidly. Their pseudopod, called lamellipod, has a characteristic 'fan'-like shape. It is few tenths of a micron thick and tens of microns long and wide. Behind the lamellipod is round cell body. The lamellipodial network mainly consists of actin regulated by a host of actin sequestering, capping, severing, nucleating, and depolymerizing proteins, and organized by crosslinking and force generating (myosin) molecules.

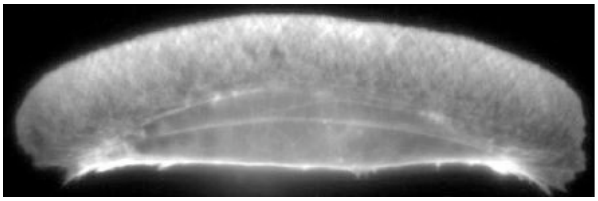

Figure 1: Actin distribution in keratocyte lamellipod. Fish keratocyte stained for Factin with rhodamine phalloidin [1].

Three mechanisms – protrusion, adhesion, and contraction – are acting in concert to produce cell movement. First, growth of the actin plus ends leads to the extension of the cell's leading edge. Then, graded adhesion of the cytoskeleton to the substrate is developed: the adhesion to the surface at the front is firmer, than at the cell's rear. Finally, the actomyosin network contracts, pulling the rear of the cell forward. In keratocytes, all these steps take place simultaneously so that the cells appear to 'glide' steadily without changing its shape.

We concentrate our computational modeling efforts on simple model systems, such as keratocytes, and also Listeria [6] and migrating amoeboid sperm of the nematode Ascaris suum [7]. In this talk we will discuss only protrusion – the best understood part of motility. There are a number of questions about actin based protrusion, where computer modeling can help: What

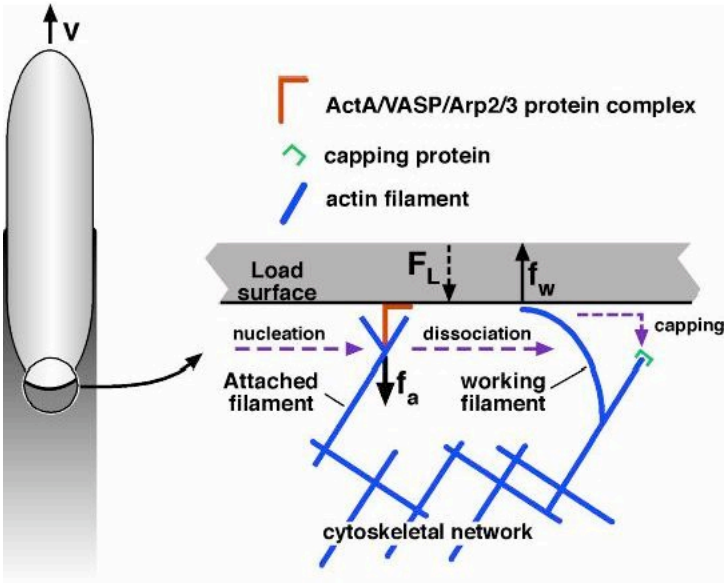

Figure 2: 'Tethered ratchet' model of protrusion force generation by Listeria actin tail [2]. The attached (straight) 'mother' filament nucleates/branches a 'daughter' filament. Dissociated 'working filaments' grow, undulate thermally and bend generating elastic force of protrusion (polymerization ratchet). Force balance between the working and attached filaments and the load explain complex force-velocity curve for Listeria. Dendritic nucleation model explains the actin tail organization and actin turnover, however, many quantitative details remain murky.

is the nature of the force of protrusion? How is actin recycled from the rear to the front of the cell? What determines the cell shape and migration speed? To answer these questions, we dissect the protrusion phenomenon and analyze first the 'tethered ratchet' model of protrusion

force generation. We apply this model to Listeria propulsion and compare its results to recent experimental data. We then discuss the model's implication for lamellipodial extension and discuss future experiments and significance of the adhesion machinery, which could be the limiting factor for protrusion.

Then, we turn our attention to the organization of actin in the lamellipod, which is explained qualitatively by the dendritic nucleation model. We examine this model quantitatively and discuss an importance of cytoplasmic convection in actin recycling. We will present preliminary results on combining 'modules' of protrusion to explain the shape and movements of the whole cell and their relations to actin dynamics and organization. We will conclude with discussing many open problems: actin network rheology in vivo, redundancy of mechanical and regulatory pathways, lack of quantitative data, and how computational modeling combined with experimental techniques could accelerate the progress in understanding cell movements.

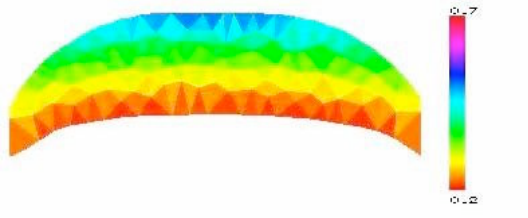

Figure 3: Preliminary results of modeling [3] of steadily migrating keratocyte lamellipodial fragments [4]. The lamellipodial actin network is modeled as a 2-D elastic domain with free boundaries. Finite element method is used to solve equations of mechanics and actin turnover and to move boundaries. Evolved fragment's shape and steady F-actin density are shown.

References:

1. H. P. Grimm, A. B. Verkhovsky, A. Mogilner, J.-J. Meister, Analysis of actin dynamics at the leading edge of crawling cells: implications for the shape of keratocyte lamellipodia. Eur. Biophys. J., In Press.

2. A. Mogilner, G.Oster (2003) Force generation by actin polymerization II: the elastic ratchet and tethered filaments. Biophysical Journal 84:1591-1605.

3. B. Rubinstein, K. Jacobson, A. Mogilner, Shape and motility of cell fragment: computational model, In Preparation.

4. A.B. Verkhovsky, T.M. Svitkina, G.G. Borisy, (1999) Self-polarization and directional motility of cytoplasm. Curr. Biol. 9:11-20.

5. A. Mogilner, G. Oster, polymer motors: pushing out the front and pulling up the back. Curr. Biol., In Press.

6. L.A. Cameron, P.A. Giardini, F.S. Soo, J.A. Theriot (2000) Secrets of actin-based motility revealed by a bacterial pathogen. Nat. Rev. Mol. Cell Biol. 1:110-119.

7. D. Bottino, A. Mogilner, T. Roberts, M. Stewart, G. Oster (2002) How nematode sperm crawl. J. Cell Science 115:367-384.

A cytoskeletal transport, assembly and signaling module during *Xenopus* oocyte wound healing

W.M. Bement, C.A. Mandato, and H.A. Benink

Cells and tissues display an astonishing array of outwardly different motility phenomena, including cell division, morphogenesis, and directed cell locomotion. Surprisingly, however, the same subset of players are involved in most, if not all of these processes: microtubules, actin filaments (F-actin), and motor molecules. To understand how identical molecules can control such apparently divergent events, we have sought to characterize basic interactions among microtubules, F-actin, and motors in several "stripped down" systems and processes. These systems, derived from *Xenopus* oocytes and eggs, include cell free extracts (1-3), inducible cortical flow in oocytes (4,5), and wound healing in oocytes (6-8). Each of these systems has specific strengths that simplify the analysis of interactions among the different cytoskeletal players, and each has been extremely useful in revealing conserved mechanisms that link these systems.

In this presentation, we will focus on our recent findings from the wound healing system. Following damage to the plasma membrane, *Xenopus* oocytes rapidly assemble a ring-like array of actin filaments and myosin-2 around the wound that is surrounded by radially-organized microtubules (Fig. 1; refs. 6-8). This array closes over time, and in so doing, drives extrusion of the damaged cell surface into the surrounding medium.

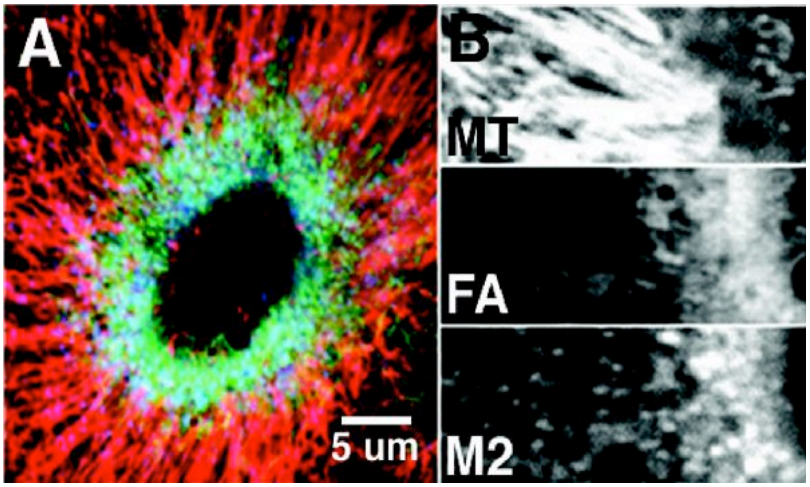

Fig. 1. A. Triple label showing microtubules (red), F-actin (green) and myosin-2 (blue) around wound made in a Xenopus oocyte. The microtubules are organized into a radial array that encloses the ring of F-actin and myosin-2B. Close up of the wound edge, showing microtubules (MT), F-actin (FA) and myosin-2 (M2) separately. Most of the microtubules terminate near the edge of the region of highest F-actin and myosin-2 density. Taken from reference 8.

4D imaging using a combination of fluorescent probes and specific manipulations of the cytoskeleton has shown that this array is generated both by assembly of actin filaments and myosin-2 in specialized zones at wound borders, as well as by myosin-driven contraction of stable F-actin to the wound border (ref. 7). Microtubules are transported to the wound borders as a result of association with moving F-actin (Fig. 2) and are also assembled at the wound border independently of the actin cytoskeleton (ref. 8).

Just as the recruitment of microtubules to the wound edge is in part due to actomyosin-based motility, the microtubules, in turn, control the local assembly of actin and myosin-2, generating a positive feedback loop. This control is exerted at least in part by microtubule-dependent control of the rho GTPases rhoA and Cdc42, as shown by the fact that RhoA and Cdc42 are rapidly activated in concentric zones around wounds and perturbation of the microtubule

cytoskeleton alters the activation pattern of these GTPases (H.A. Benink and W.M. Bement, unpublished results).

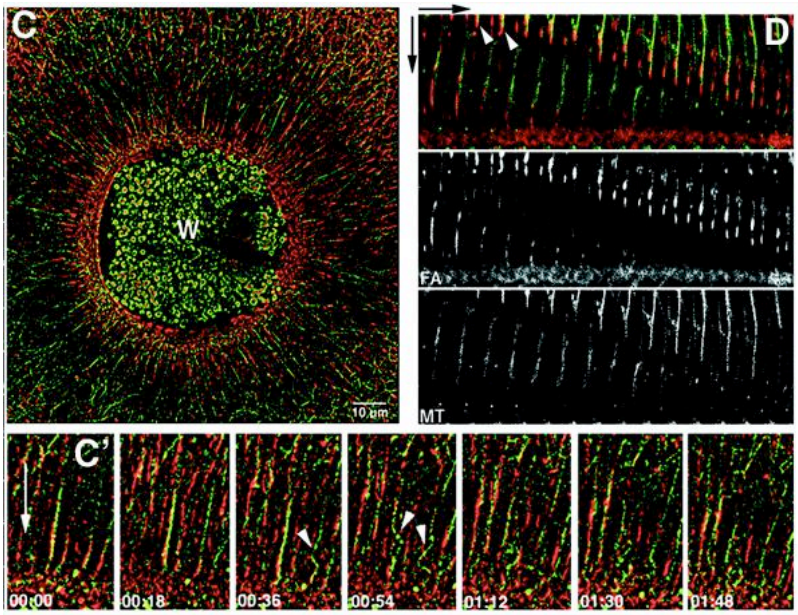

Fig. 2. Images from 4D movies showing transport of microtubules (green) by F-actin (red) during wound healing. C is a low mag picture provided for orientation while C' and D provide higher magnification views of the transport process. Microtubules move toward wound (downward arrows) in association with F-actin (C', D) and buckle as they hit the actin-rich region at the wound edge (arrowheads, C'). Taken from reference 8.

Many of the processes observed during oocyte wound healing are consistent with proposed models of cytokinesis (9), and bear remarkable similarity to those occurring during cell locomotion (10), providing strong support for the notion that diverse cell motility events can be underlain by conserved cytoplasmic activity modules (Fig. 3). In this case, the activity module is comprised of actomyosin-dependent transport of microtubules toward the wound edge, complemented by microtubule-dependent assembly of F-actin and myosin-2 around wound borders.

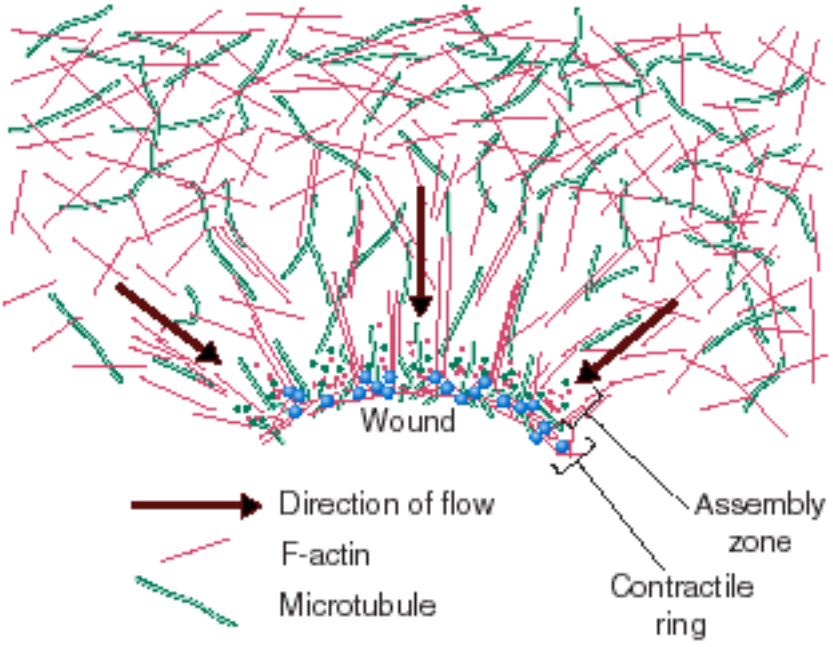

Fig. 3. Schematic showing wound healing "activity module". Taken from ref. 10

References:

1. J.R. Sider, C.A. Mandato, K.L. Weber, A.J. Zandy, D. Beach, R. Finst, J. Skoble and W.M. Bement. Direct observation of microtubule f-actin interactions in cell free lysates. 1999. J. Cell Sci. 112:1947-1956

2. C.M. Waterman-Storer, D.Y. Duey, K.L. Weber, J. Keech, R.E. Cheney, E.D. Salmon, and W.M. Bement. 2000. Analysis of microtubule/f-actin interactions in *Xenopus* egg extracts reveals two mechanisms of microtubule-dependent f-actin motility. J. Cell Biol. 150:361-376.

3. K.L. Weber and W.M. Bement. Actin serves as a template for cytokeratin assembly in cell free extracts. 2002. J. Cell Sci. 115:1373-1382.

4. J.C. Canman and W.M. Bement. Microtubules suppress actomyosin-based cortical flow. 1997. Microtubules suppress actomyosin-based cortical flow in *Xenopus* oocytes. J. Cell Sci. 110:1907-1917.

5. H.A. Benink, C.A. Mandato, and W.M. Bement. 2000. Testing models of cortical flow in vivo. Mol. Biol. Cell 11:2553-2563.

6. W.M. Bement, C.A. Mandato and M.N. Kirsch. 1999. Wound-induced assembly and closure of an actomyosin purse string in *Xenopus* oocytes. Curr. Biol. 9:579-587.

7. C.A. Mandato and W.M. Bement. 2001. Contraction and polymerization cooperate to assemble and close actomyosin rings around *Xenopus* oocyte wounds. J. Cell Biol. 154:785-798.

8. C.A. Mandato and W.M. Bement. 2003. Actomyosin transports microtubules and microtubules control actomyosin recruitment during oocyte wound healing. Curr. Biol. 13:1096-1105.

9. C.A. Mandato, H.B. Benink, and W.M. Bement. 2000. Microtubule-actomyosin interactions during cortical flow and cytokinesis. Cell Motil. Cytoskel. 45:87-92.

10. O.C. Rodriguez, A.W. Schaefer, C.A. Mandato, P. Forscher, W.M. Bement and C.M. Waterman-Storer. 2003. Conserved microtubule-actin interactions in cell movement and morphogenesis. Nature Cell Biol. 5:599-609.

Microtubule/actin interaction modules in directed cell locomotion

Clare M. Waterman-Storer

Although it is certainly true that microtubules and actin play distinct roles in cells, it has been evident for some time that interactions between these seemingly distinct filament systems exist. Vasiliev hinted at this years ago when he showed in migrating fibroblasts that maintenance of the polarized distribution of actin-dependent protrusion at the leading edge

required an intact microtubule cytoskeleton. Microtubules and actin exhibit two mechanistic classes of interactions, "Regulatory Interactions" in which Rho-family signaling cascades co-regulate microtubules and actin, and whose activity is spatiotemporally controlled by microtubules, and "Structural Interactions" in which actin and microtubules are physically cross-linked. RhoA mediates formation of contractile actin bundles and microtubule stabilization, Rac1 activates polymerization of both actin and microtubules to promote lamellipodial protrusion, while Cdc42 mediates actin bundle polymerization into filopodia and directs the positioning of the microtubule organizing center (MTOC) in migrating cells. At the same time, microtubule disassembly activates RhoA while microtubule assembly promotes Rac1 activation. Recent in vivo and in vitro studies show that structural interactions between microtubules and actin result in an interdependence of their dynamic organization in migrating cells. Analysis of actin and microtubules by dual-wavelength FSM showed that microtubules are coupled to actin retrograde flow in the lamella, and to anterograde motion of actin in the cell body (Figs. 1,2). Microtubules also grow along actin bundles towards focal adhesions, and microtubule ends often are dragged through the cytoplasm by their connection to moving actin bundles.

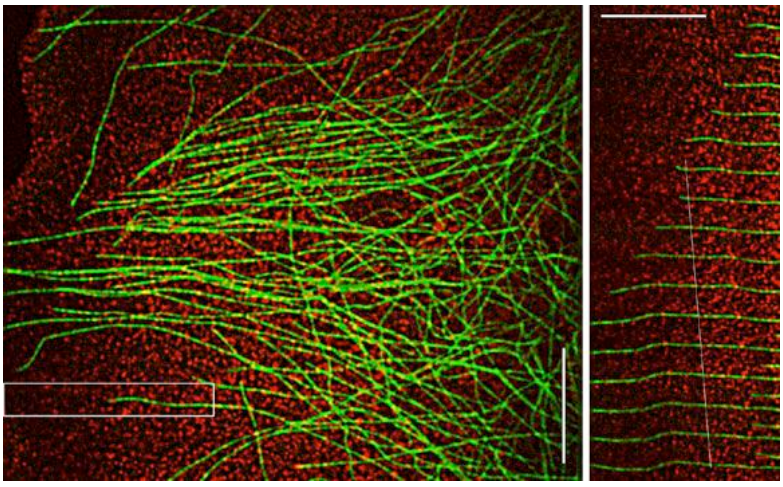

Fig 1. Microtubules and F-actin movements are coupled in the lamellum of a migrating newt lung epithelial cell. (A) FSM image, leading edge is at the left. (B) Time montage of the boxed region in the upper panel. The microtubule is transported rearward while simul-taneously growing towards the leading edge. The white line tracks a speckle on the microtubule, which is moving at the same velocity as speckles in the actin meshwork. Bar = 10 mm.

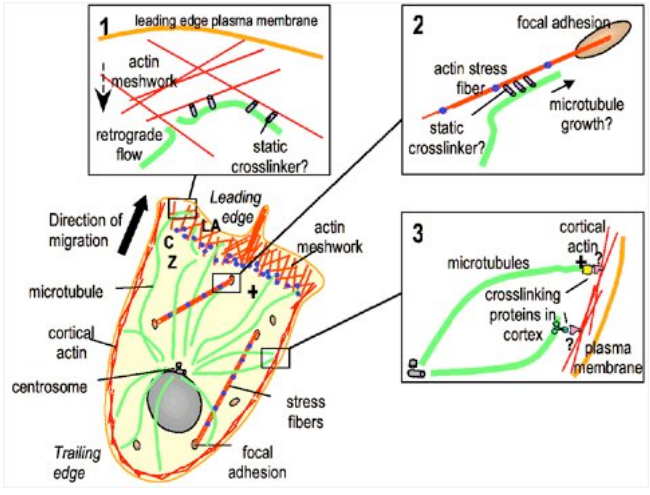

Fig. 2. In migrating tissue cells, microtubule (green) minus ends are organized by the centrosome, which is positioned between the nucleus and the leading edge, and their plus ends are toward the leading edge. In lamellipodia (LA), F-actin (red) is in a meshwork that undergoes retrograde flow towards the convergence zone (CZ) where myosin contraction (blue dots) is concentrated. Stress fibers are contractile acto-myosin bundles with their ends anchored in focal adhesions. Insets: putative microtubule-actin interactions in different regions of a migrating cell. (1) In the lamellum, microtubules are coupled to F-actin undergoing retrograde flow, compressing and breaking microtubules to promote regional microtubule turnover. (2) Microtubules could target focal adhesions by cross-linking to and growing along focal adhesion-associated actin bundles. (3) Microtubule plus ends may be anchored at the cell cortex via interactions between plus-end binding proteins and actin binding proteins to orient the MTOC towards the direction of migration.

How do these interactions mediate cell movement? One hypothesis is that cell motility depends on the structural linkage of microtubules to actin retrograde flow, which in turn establishes and maintains a signaling gradient that perpetuates motility. Constant microtubule retrograde flow requires compensatory net growth towards the leading edge. Behind the lamellum, microtubule breakage and depolymerization occurs as a result of the compressive forces of the contracting actin to which they are bound. Thus, linkage of microtubules to regional actin movements results in a gradient of microtubule assembly states in the cell with growth at the leading edge and shortening behind the lamellum. Microtubule growth could promote local activity of Rac1 in the cell front to drive lamellipodial protrusion and perpetuate further microtubule growth, while microtubule shortening could activate RhoA behind the lamellum to drive actomyosin contraction and promote the stabilization of a subpopulation of microtubules, possibly to protect them from breakage and thus maintain the overall polarization of the microtubule cytoskeleton. We call this the "polymerization/contraction treadmill module" (Fig 3a) and we will discuss how it appears to be conserved for use in other cellular environments where gradients in polymerization and contraction must be perpetuated.

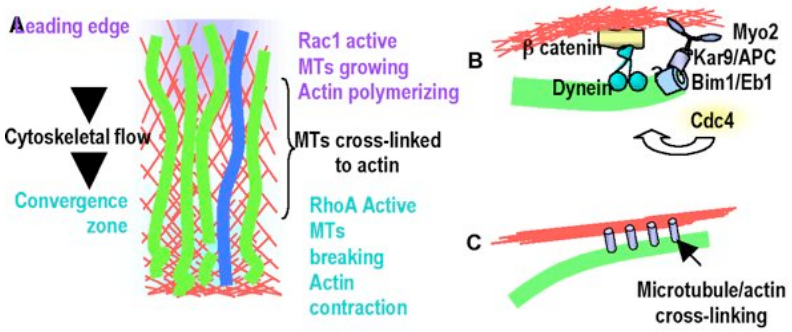

Fig. 3. Microtubule-actin interaction "activity modules." (A) The "polymerization/contraction treadmill" module. At the leading edge Rac1 activity stimulates actin and microtubule polymerization, and is perpetuated by microtubule growth. Microtubules (green) crosslinked to actin (red) undergo retrograde flow. As they approach the region of actin contraction, they buckle, break and depolymerize. Microtubule disassembly activates RhoA to perpetuate contraction and stabilization of a subset of microtubules (blue). (B) The "plus end/cortex anchor" where stable attachment of microtubules to the actin cortex via a plus-end complex is directed by Cdc42. (C) The "actin bundle/microtubule guidance" module may be important for precise positioning of microtubules at focal adhesions.

Alternatively, structural and regulatory microtubule/actin interactions may mediate specific spatiotemporal regulation of focal contacts with the substrate to guide cell motility Microtubules may bind to and grow along actin filament bundles to precisely deliver a signal that promotes focal adhesion disassembly (Fig 2.2). We call this the "actin bundle/microtubule guidance module" (Fig 3c), and will discuss how it may be used in situations where the targeting of single microtubules to precise positions is required.

Finally, microtubule/actin interactions could orient microtubules towards the leading edge, which could direct the delivery of signaling molecules or membrane components required for lamellipodial protrusion. Recent evidence suggests that Cdc42-mediated MTOC reorientation may occur by "capture" of microtubule ends by the actin cortex, where cytoplasmic dynein motors pull the cytoplasmic microtubule complex into position. We call this the "plus end/cortex anchor module" and will discuss how it may be conserved in processes that require asymmetric microtubule distributions in a variety of cellular contexts and functions. (Fig. 3b).

References:

Rodriguez, O., A. Schaefer, C.M. Mandato, P.M. Forscher, W.M. Bement, and C.M. Waterman-Storer (2003) Dynamic microtubule-actin interactions: Conserved mechanisms underlying directed cell movement and polarized morphogenesis. Nat. Cell Biol. 7:599-609

Wittmann, T. and C.M. Waterman-Storer (2001) Cell motility: can Rho GTPases and microtubules point the way? J. Cell Sci. 114, 3795-803

Wittmann, T., G.M. Bokoch, and C.M. Waterman-Storer (2003) Co-regulation of leading edge microtubule and actin dynamics downstream of Rac1 and Pak1. J. Cell Biol. 161:845-51

Waterman-Storer, C.M., R.A. Worthylake, B.P. Liu, K. Burridge, and E.D. Salmon (1999) Microtubule growth activates Rac1 to promote lamellipodial protrusion in fibroblasts. Nat. Cell Biol. 1:45-50

Salmon, W. C., M.C. Adams, and C.M. Waterman-Storer (2002) Dual-wavelength fluorescent speckle microscopy reveals coupling of microtubule and actin movements in migrating cells. J. Cell Biol. 158:31-7

Gupton, S. L., W.C. Salmon, and C.M. Waterman-Storer (2002) Converging populations of f-actin promote breakage of associated microtubules to spatially regulate microtubule turnover in migrating cells. Current Biology 12:1891-99

Somatic budding in *Drosophila* / cytokinesis in sea urchins

George von Dassow and Victoria Foe

The mechanisms by which cells initiate cytokinesis remain poorly-understood. Unsolved questions include: how the mitotic apparatus communicates its position to the cell surface; what pre-existing structure, if any, assembles into the contractile ring; and what determines the time of furrowing? Historically, biologists have sought to reconcile conflicting observations on diverse cells into a unified explanation of animal cell cytokinesis. Even so neither of the two popular textbook stereotypes - polar relaxation or equatorial stimulation - matches more than half the known facts about the process. Indeed, even isolated cells are so diverse in form, size, timing, mechanics, etc. that any one-size-fits-all mechanism strains credibility. There is a wealth of variation in cytokinesis among animal embryos; some of these natural experiments are shown in Figure 1. Recent experiments confirm that cells differ in fundamental aspects of cytokinesis; for example, while Rappaport's experiments with sand dollar eggs showed that juxtaposition of two mitotic asters suffices to induce a furrow, recent results suggest that spindle mid-zone microtubules stimulate furrowing in mammalian cells, and new observations on frog eggs suggest a role for cortical, i.e. non-spindle and non-astral, microtubules.

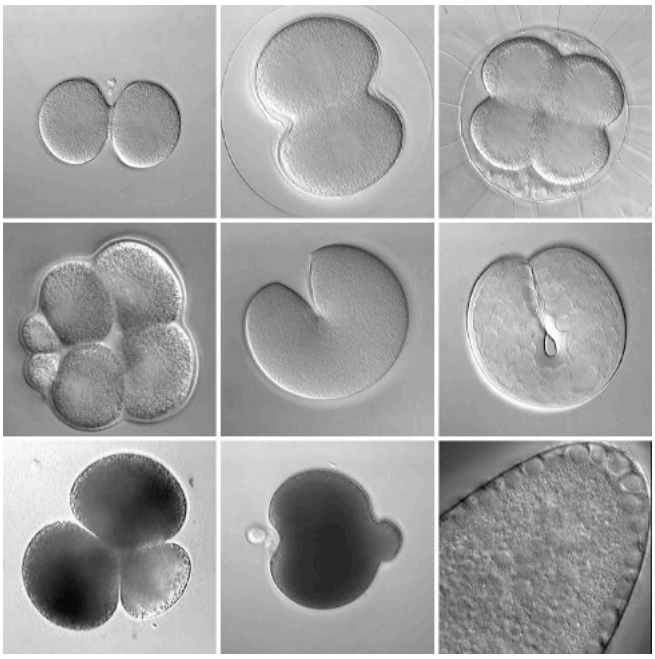

Figure 1: Various embryos during early cleavage. Top row: normal cytokinesis in the nemertean Cerebratulus (left), the urchin S. droebachiensis (middle), and the ascidian Corella (right). Middle row: variations on cytokinesis include unequal cleavage in urchin embryos (left; the urchin S. purpuratus), and "unipolar" cytokinesis in the embryonic cells of cnidarians (middle; the jellyfish Aequorea) and ctenophores (right; Pleurobrachia). Bottom row: cytokinesis-like processes include polar lobe formation in diverse spiralians including scaphopods (left; Pulsellum) and bivalves (middle; the clam Acila), and somatic budding (right; the wasp Nasonia). All panels are DIC images taken from time-lapse movies.

We got interested in cytokinesis during studies on two aspects of syncytial development in *Drosophila*. One of us studied nuclear migration during early mitoses, finding that astral microtubules locally re-organize a cytoplasmic actin network; this local change stimulates bulk cytoplasmic streaming until nuclei achieve a uniform distribution. The other studied bud formation at a slightly later stage, after nuclei arrive at the cortex of the syncytium but prior to cellularization, and concluded that pseudo-cleavage furrows arise from directional movement of cortical actin and myosin II along astral microtubules (for 3-D reconstructions describing the cytoskeleton during bud formation, visit DownTheTubes). We wondered whether these two phenomena, which otherwise seem like oddities of syncytial development, might share homologies to classical cytokinesis (see Foe et al. 2000).

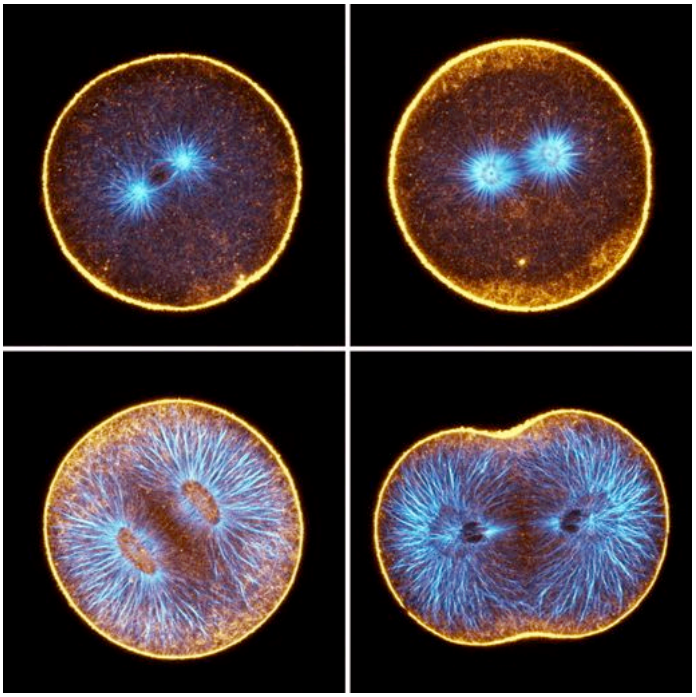

Figure 2: Confocal sections of sand dollar embryos in first cleavage; orange=F-actin, blue=microtubules. Top left: prophase; during interphase and prophase, we detect very little F-actin in the deep cytoplasm. Top right: metaphase; cytoplasmic F-actin becomes apparent in metaphase. Sometimes, as shown here, the deep actin network first appears as an annulus around the cleavage plane. Bottom left: mid-anaphase; the deep actin network is most prominent during anaphase, but the density of F-actin is roughly complementary to the density of microtubules. Bottom right: telophase; the deep actin network disappears progressively during cleavage, and remains longest in the furrow zone.

We are examining the configuration of microtubules, F-actin, and myosin during cyokinesis in early sea urchin embryos, and find much in common despite the very different geometrical context. Early urchin embryos, like early fly embryos, make an extensive cytoplasmic actin network during mitosis, which all but disappears by the end of cleavage (Fig. 2). The actin network appears to be re-organized by astral microtubules. As in fly embryos, myosin II disappears from the cortex and then is recruited to the furrow region in phase with the cell cycle. We are also investigating the unequal fourth cleavage in urchin embryos. At the end of third cleavage, the vegetal cortex apparently captures one of the two centrosomes, leading to spindle displacement and re-orientation (Fig. 3). The cortically-located spindle pole forms a flattened aster, at the edge of which the cleavage furrow forms. This is reminiscent of pseudocleavage furrowing in *Drosophila*, except that in this case complete cleavage results.

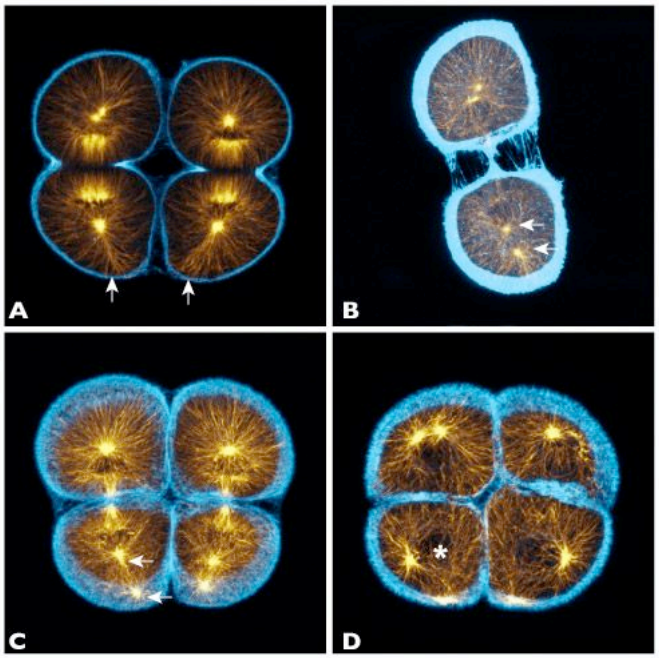

Figure 3: Projections of 10-20 confocal sections of purple urchin embryos near the end of third cleavage; orange = microtubules, blue = F-actin. Top left: telophase; as the cells cleave, we observe a loose bundle of microtubules, prominent against the rest of the aster, that reaches the vegetal cortex (arrows). Top right: late telophase; one of the two nascent MTOCs (arrows) in the vegetal daughter becomes displaced away from the nucleus. Bottom left: early interphase; the displaced MTOC migrates to the vegetal cortex, while the other remains associated with the re-forming nucleus. Bottom right: interphase; once the nucleus reforms near the cell center (asterisk), it subsequently migrates into position between the two MTOCs.

Our goal is to characterize a tool-kit of homologous processes which all cells likely share, and investigate how those cytomechanical modules have been deployed and weighted differently to accomplish diverse modes of cell cleavage and cleavage-like phenomena. That is, rather than pursuing the One True Mechanism, we suspect it will be more realistic to explain cytokinesis in terms of conserved sub-processes with different contributions in different contexts.

References:

von Dassow G, Schubiger G. (1994) How an actin network might cause fountain streaming and nuclear migration in the syncytial *Drosophila* embryo. J Cell Biol. 127:1637-53.

Foe VE, Field CM, Odell GM. (2000) Microtubules and mitotic cycle phase modulate spatiotemporal distributions of F-actin and myosin II in *Drosophila* syncytial blastoderm embryos. Development 127:1767-87.

Cell polarity: polarization of the *C. elegans* zygote along the anterior-posterior axis

Geraldine Seydoux

We are interested in the mechanisms that generate asymmetries within cells and are using the *C. elegans* zygote as a model system. *C. elegans* zygotes are relatively large, optically clear eggs, which can complete embryogenesis on a microscope slide. Unlike other commonly studied eggs, which develop molecular asymmetries during oogenesis, *C. elegans* eggs first become polarized after fertilization using cues that arise in the egg itself. In particular, polarity along the anterior-posterior (A/P) axis is determined by the sperm asters, whose position specifies the posterior end of the embryo. In response to this cue, cortical contractions cease in the posterior and several cortically-enriched PAR proteins relocalize to non-overlapping anterior and posterior domains. The PAR proteins in turn regulate the asymmetric distribution of cell fate determinants in the cytoplasm. Polarization takes <10 minutes and is easily followed by time-lapse microcopy.

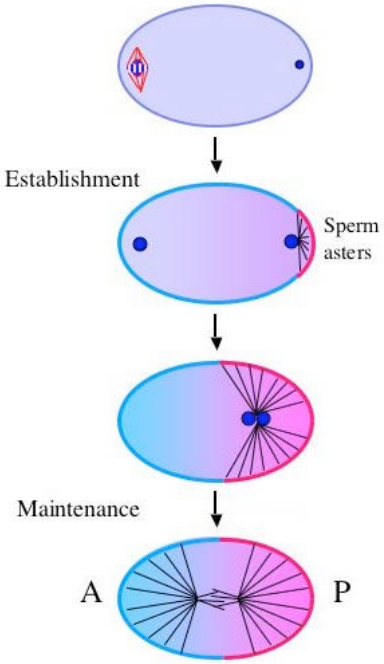

Figure 1

We focus on several questions, in particular:

1) How is the transient cue provided by the sperm asters transformed into a stable axis maintained through cleavage?

Using GFP fusions to follow polarization dynamics in live embryos, we found that polarization involves two genetically and temporally distinct phases (ref 1). During the first phase (establishment), local interactions between the sperm asters and the actin rich cortex exclude the "anterior" PAR proteins (blue in Fig. 1), allowing the "posterior" PAR protein PAR-2 (pink) to accumulate in an expanding domain on the cortex nearest the asters. The second phase begins when the asters assemble the mitotic spindle and begin to invade the anterior. During this phase (maintenance), PAR-2 maintains anterior-posterior polarity by excluding the anterior PARs from the posterior. These findings suggest that PAR-2 plays an essential role in transforming the transient cue from the sperm asters into a stably polarized axis. PAR-2 is a novel protein with a ring finger and an ATP binding site, and we are currently investigating which of these domains are required for function.

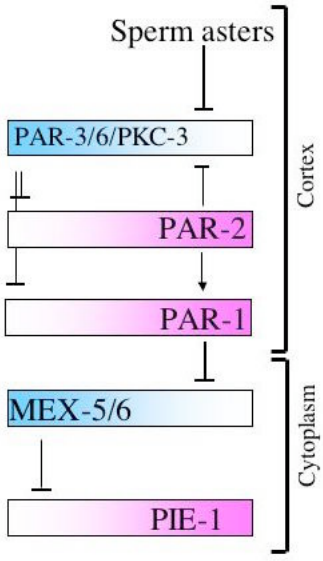

Figure 2

2) How do proteins become asymmetrically localized?

Studies in the Kemphues and Priess labs have led to a "sequential repression" model (Fig. 2) to describe the hierarchy of genetic interactions that restrict specific proteins to the

anterior or posterior. Anterior PARs and posterior PARs mutually exclude each other. Posterior PARs locally exclude MEX-5 and MEX-6, which in turn exclude PIE-1 and other germline proteins from the anterior (Fig. 3).

Using GFP transgenes, we have begun to define domains required for localization. Our results so far suggest that asymmetric protein localization in *C. elegans* zygotes depends mostly, if not entirely, on post-translational mechanisms.

In the case of PIE-1, we identified two complementary mechanisms required for localization: a first (still poorly understood) mechanism which causes PIE-1 to become enriched in the posterior half of the zygote before cleavage, and a second mechanism which degrades any protein left over in the anterior after cleavage. The latter is mediated by a novel E3 ubiquitin ligase, which recognizes a unique CCCH finger motif in PIE-1 (ref 2). Degradation is activated in anterior cells by MEX-5 and MEX-6 and inhibited in posterior cells by PAR-1.

These findings have led us to wonder whether localized protein degradation could also be driving asymmetry in the zygote. I will speculate on the possibility that local changes in protein stability between competing proteins may be the dominant mechanism driving asymmetric localization in *C. elegans* zygotes.

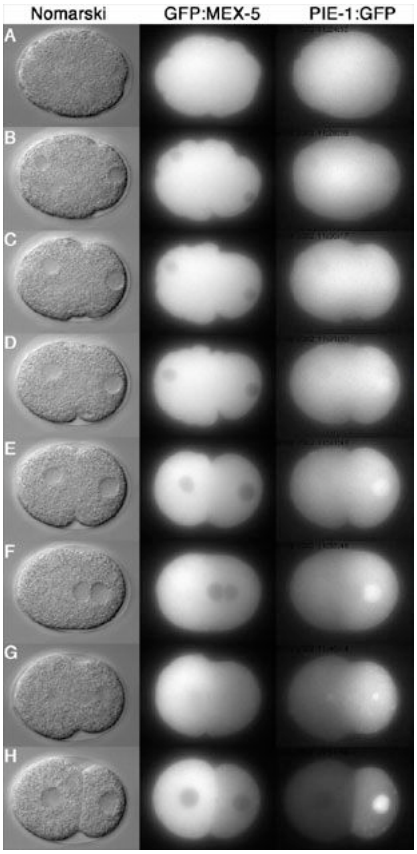

Figure 3

References:

1. Cuenca, A., Schetter A. , Aceto D., Kemphues K., Seydoux, G. (2003). Polarization of the *C. elegans* zygote proceeds via distinct establishment and maintenance phases. Development 130, 1255-1265.

2. Derenzo, C., Reese, K. and Seydoux, G. (2003). Exclusion of germ plasm proteins from somatic lineages by cullin-dependent degradation. Nature, advance on line publication July 23 2003.

Asymmetric cell division in the developing CNS

Andrea Brand

A simple way to generate two different cell types upon division is through the asymmetric segregation of cell fate determinants, a mechanism that is used in organisms as widely divergent as bacteria and mammals. Asymmetric segregation is used in yeast to distinguish mother cells from their daughters, and in C. elegans, to differentiate the sister cells arising from the first embryonic division. Asymmetric cell division is also observed in the developing

nervous system of both vertebrates and invertebrates. In the Drosophila nervous system, a number of cell fate determinants segregate to the GMC upon division. One is the homeodomain transcription factor, Prospero, named after the wizard who controls the fate of the other characters in Shakespeare's "The Tempest". Prospero activates GMC-specific genes such as even-skipped and ftz and represses neuroblast-specific genes such as asense and deadpan.

The asymmetric localisation of determinants is an elegant mechanism for rapidly switching from a stage of proliferation, when similar daughter cells are born (Figure 1, left), to a stage of diversification, when different daughter cells are generated (Figure 1, right). For example, in epithelial cells Prospero localises basolaterally but is segregated equally to both daughter cells at division. Neuroblasts also localise Prospero basally but, as they divide perpendicular to the epithelial layer, only one of the daughter cells inherits Prospero. Coordination of the mitotic spindle with the apico-basal axis of the cell appears to be a prerequisite for successful asymmetric segregation. We have shown that during pro/metaphase the neuroblast mitotic spindle rotates 90°, so as to align itself along the apico-basal axis of the cell and asymmetrically segregate Prospero.

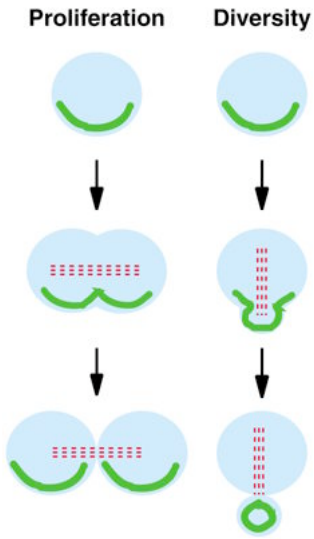

Figure 1

Prospero protein is localized to the basal cortex of neuroblasts by the adapter protein Miranda, a novel coiled-coil protein (named after Prospero's daughter in The Tempest). Prospero mRNA is also basally localised. Miranda binds directly to Prospero protein and also, we have shown, to Staufen, a double-stranded RNA binding protein, which in turn binds prospero mRNA. When neuroblasts divide, only the basal daughter cell (the GMC) inherits Miranda and its cargo of Prospero protein and prospero mRNA. Miranda then releases Prospero protein, which translocates to the GMC nucleus.

Role of Cytoplasmic Myosin II in Asymmetric Cell Division:

F-actin appears to play a key role in the asymmetric localisation of cell fate determinants in yeast and worms. Similarly, in Drosophila when F-actin is depolymerised by treatment with latrunculin, Prospero is released from the cortex. The mechanism by which Prospero (and its adapter Miranda) localise to the basal half of the cell cortex is unclear, as F-actin is uniformly distributed around the cortex.

The dynamics of asymmetric localisation and the dependence on F-actin suggest a role for myosin motor proteins in asymmetric cell division. We have found that cytoplasmic Myosin II, or Zipper, plays an integral role in localising determinants in neuroblasts. Myosin II is the homologue of C. elegans NMY-2, which is required to localise PAR proteins

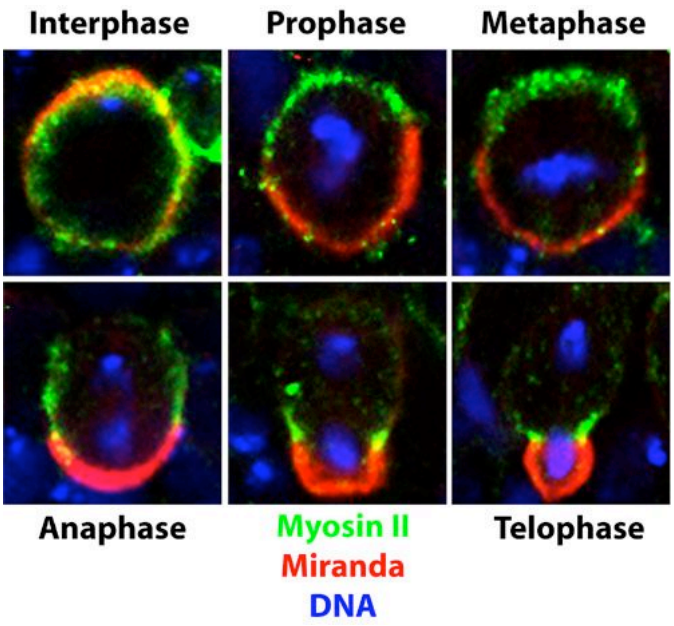

Figure 2

asymmetrically at the cortex of the one-cell embryo, revealing a conserved role for myosin II motors in mediating actin-dependent asymmetric segregation. Myosin-II has also been shown also to localise b-actin mRNA to the leading edge of fibroblasts.

In contrast with NMY-2, which is localised uniformly around the cortex of the worm zygote, we find that Drosophila Myosin-II is asymmetrically localised in neuroblasts (Figure 2). Interestingly, Miranda and Myosin do not overlap extensively in neuroblasts. As Myosin moves to the cleavage furrow during anaphase and telophase, it appears to "push" Miranda into the GMC. I would like to discuss the possible mechanisms by which Myosin-II is localised, and the means by which Myosin might localise Miranda. One clue is that Drosophila Myosin-II interacts directly with the tumour suppressor, Lethal giant larvae. In yeast, the Lgl counterparts Sro7p and Sro77p exhibit strong genetic interactions with the myosins Myo1 and Myo2. Lgl is itself required for asymmetric cell division in neuroblasts and in yeast has a role in exocytosis.

References:

Schuldt, A.J., Adams, J.H.J., Davidson, C.M., Micklem, D.R., Haseloff, J., St. Johnston, D. and Brand, A.H. (1998). Miranda mediates asymmetric protein and RNA localisation in the developing nervous system. Genes and Development, 12, 1847-1857.

Kaltschmidt, J.A., Davidson, C.M., Brown, N.H. and Brand, A.H. (2000). Rotation and asymmetry of the mitotic spindle direct asymmetric cell division in the developing central nervous system. Nature Cell Biology, 2, 7-12.

Barros, C.S., Phelps, C.B. and Brand, A.H. Drosophila non-muscle myosin II promotes the asymmetric segregation of cell fate determinants (in preparation).

Cell-cell adhesion and cell polarity

Soichiro Yamada and W. James Nelson

The long term goals of our work are to understand how epithelial cells organize into monolayers through specialized cadherin-mediated cell-cell contacts, and localize proteins to functionally different plasma membrane domains. We integrate different experimental approaches to address these problems: structural analysis of proteins and protein complexes, high resolution live cell imaging, biochemical analysis of protein complex assembly and function in cells, and in vitro reconstitution of protein functions. We have defined stages in cell-cell adhesion and obtained preliminary evidence of a mechanism involved, determined how several plasma membrane proteins are targeted to and organized in specific membrane domains, and developed new in vitro methods to dissect protein interactions and functions at cell-cell contact plasma membranes. controlling membrane domain formation by cadherin-based cell-cell adhesions. These results begin to define molecular linkages and mechanisms controlling membrane domain formation by cadherin-based cell-cell adhesions.

We discuss 3 experimental approaches, each providing a different angle of insight into protein localization, interactions and, potentially, function. Our aim is to combine the overlapping

information derived from each approach to generate a more complete picture, and to use information obtained from one approach to design new experiments using another approach.

Regulation of cadherin and actin cytoskeleton organization during cell-cell adhesion [live cell imaging]:

We use high resolution, time-lapse imaging and FRAP analysis of GFP fusion proteins (e.g., E-cadherin, actin, Rac1, PH-AKT, etc) to describe stages in cell-cell adhesion, and then mutant proteins and pharmacological interventions to investigate underlying mechanisms. We find that as migratory MDCK cells collide, lamellipodia increase in number, perdurance and concentration at cell-cell contacts, coincident with localization of Rac1 and PH-AKT (marker for PI(3,4,5)P3) at edges of the expanding contact, indicating that cadherin engagement results in local activation of Rac1, perhaps through recruitment of GEFs. Immediately, a highly mobile, diffuse pool of E-cadherin coalesces between contacting membranes into immobile puncta that are spatially coincident with membrane attachment sites for actin filaments (Fig. 1). Subsequently, circumferential actin cables underneath the forming contact separate (Fig. 1), and the resulting ends of the cable together with a subset of E-cadherin puncta are swept laterally resulting in gradual maximization of the contact length. Based on studies with inhibitors of Rho-kinase (Y27632) and MLCK (ML-7), RhoA activation of actin-myosin contraction at the edges of thee contact may be important for this later stage of cell-cell adhesion that lead to compaction.

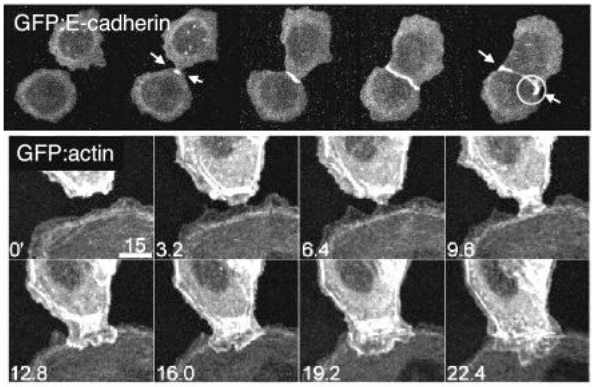

Figure 1: Time-lapse fluorescence microscopy of MDCK cells expressing E-cadherin/GFP (top) or actin/GFP (bottom) at different times during cell-cell adhesion.

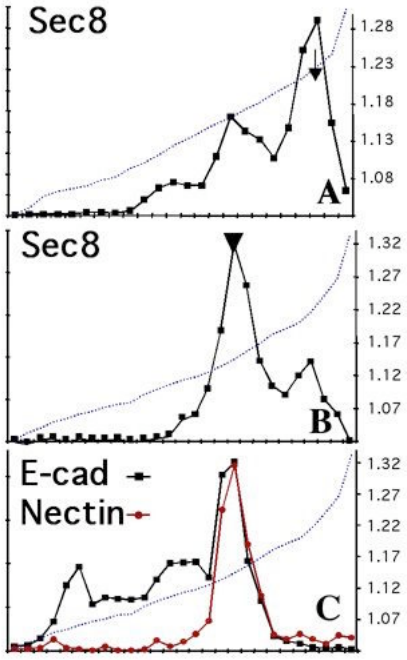

Figure 2: MDCK membranes separated in OptiPrep gradients (self-forming from a 10-20-30% step gradient) 6hrs (A) and 48hrs (B, C) after cell-cell adhesion; after SDS-PAGE, western blotting showed recruitment of Sec8 from a large cytosolic pool (arrow) to membranes containing adhesion proteins E-cadherin and nectin (arrowhead).

Junctional complex assembly, and assembly of the targeting patch (Sec6/8 complex) [biochemical analysis]:

E-cadherin-mediated cell-cell adhesion leads to the rapid formation of a new membrane domain at the site of contact, and the eventual development of cellular polarity. Formation of a new membrane domain, apical or basal-lateral requires targeting of transport vesicles from the

Golgi to that membrane domain. We focused on the link between cell-cell adhesion and formation of a targeting patch to specify basal-lateral vesicle delivery to that site. The exocyst/Sec6/8 complex is a multi-protein complex essential for targeting exocytic vesicles to specific docking sites on the plasma membrane of polarized epithelial cells. E-cadherin-mediated cell-cell adhesion results in rapid recruitment (t1/2 3-6 h) of ~70% of the Sec6/8 complex to sites of cell-cell contact. To examine protein complexes involved in Sec6/8 recruitment, we have been able to fractionate membrane microdomains in OptiPrep density gradients, resulting in the separation of apical membranes, tight junctions, and the remainder of the lateral membrane (Fig. 2 shows distributions of Sec6, E-cadherin and nectin at early (6hrs) and late (48hrs) times after cell-cell adhesion; note change in Sec8 distribution to membranes containing nectin and E-cadherin). Protein complexes can be further resolved by solubilizing membranes in detergent-containing buffer, and proteins identified directly by immunoprecipitation and western blotting, or following a subsequent separation step by Superose 6 FPLC. The combination of these approaches has lead to the identification of E-cadherin and nectin 2a as membrane binding sites for the Sec6/8 complex. This consistent with the requirement for cadherin-mediated adhesion in both recruited of the complex to sites of cell-cell adhesion, and studies for other laboratories showing that cadherin-mediated adhesion leads to delivery of basal-lateral transport vesicles to those membrane sites.

Mechanisms of assembly/function of actin and microtubule cytoskeletons after cell-cell adhesion [in vitro reconstitution]:

While there has been progress in identifying protein complexes and correlating activities with events at cell-cell contacts, we are still limited in our ability to biochemically define protein assembly pathways and functions. We have developed and characterized a new method that will enable us to reconstitute and molecularly dissect cytoskeleton (catenins, actin filaments) and targeting patch (Sec6/8 complex, SNARE proteins) assembly and function at E-cadherin-mediated adhesion sites. The basis for this method is the attachment of MDCK cells to a correctly oriented dense E-cadherin substrate and the in situ isolation of open lateral plasma membrane patches attached to the E-cadherin substratum. Dense, correctly oriented and functional E-cadherin substratum is prepared as described in Fig.3. MDCK cells rapidly attach, spread using lamellipodia, and flatten on the FcE-cadherin substratum within ~5hrs (Fig. 4, top). Immunofluorescence shows that cell-FcE-cadherin bound membrane contains proteins characteristic of lateral membranes (E-cadherin, catenins, ZO-1, Na/K-ATPase, fodrin, Sec6/8 complex), but not of basal (paxillin, integrins) or apical (gp135) membranes.

To prepare open lateral plasma membrane patches, cells are treated to a short sonication pulse which shears off apical membranes, nuclei and intracellular organelles, leaving behind open lateral plasma membrane patches attached to the FcE-cadherin substratum. Lateral plasma membrane patches labeled with the lipid dye DiI show a characteristic, homogeneous patch-like pattern (Figure 4), and staining with E-cadherin and catenins and other proteins characteristic of the lateral membrane (not shown) domain reveal punctate and diffuse staining over the patches. Membrane-associated proteins such as actin/a- and b-catenin are stripped from membrane patches with 4M guanidine-HCl, but membrane

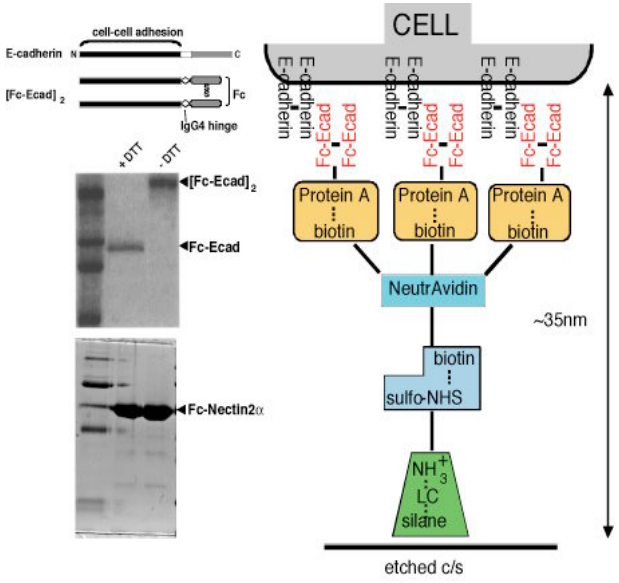

Figure 3: Preparation of FcE-cadherin substrate.

patches and E-cadherin remain intact (Fig. 4). Incubation with cytosol leads to the re-addition of a- and b-catenin to E-cadherin sites (Fig. 4); note that E-cadherin cytoplasmic domain is naturally unstructured, and adopts an ordered secondary structure only after binding to b-catenin. Incubation of lateral membrane patches with fluorescein-labeled G-actin leads to formation of long actin filaments that appear to originate from E-cadherin/catenin clusters (Fig. 4). Protein complexes have now been assembled from purified proteins.

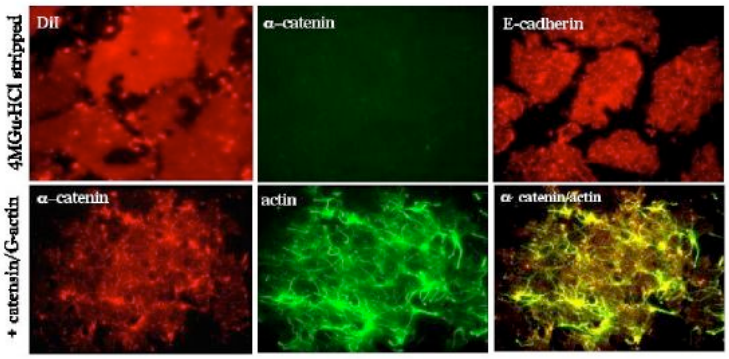

Figure 4: Immunofluorescence of MDCK lateral membrane patches attached to EcadFc substratum. Top, Patches were stripped with 4M guanidine-HCl, note patches are intact (DiI), stripped of a-catenin (center), but transmembrane E-cadherin (right) remains; Bottom, Stripped patches were incubated with cytosol as a source of catenins which bind (left) to E-cadherin (not shown), and then Fl-labeled G-actin (center) was added at RToC for 15', note actin filaments have polymerized and appear to be concentrated at membrane spots of reconstituted (a-) catenins/E-cadherin complexes (right).

We have adapted these techniques further: 1). Basal membrane patches attached to extracellular matrix to study microtubule-plasma membrane interactions and organization; 2). Imaging and biochemical manipulation of exocytic transport vesicle docking and fusing with cadherin-based membrane patches (role of Sec6/8 complex and syntaxin); 3). Formation of micro-patterned chimeric substrata containing extracellular matrix surrounding fixed or lipid bilayer supports containing cadherin.

Physical mechanisms in morphogenesis and their application to organ printing

Gabor Forgacs

Self-assembly is the fundamental process, which generates structural organization across scales both in living and inanimate systems. Morphogenesis, an example of self-assembly characterizes early development when through cell-cell and cell-extra cellular matrix interactions the developing organism and its parts gradually acquire their final shape. Morphogenesis is under strict genetic control. However genes do not give rise to forms and shapes, physical mechanisms do. Therefore it is obvious that physical mechanisms, in particular those typical for viscoelastic materials, must play crucial role in the characteristic self-assembly machinery shaping the embryo.

The present talk is a short overview of biomechanics, the discipline that deals with the viscoelastic properties of biological materials. We will concentrate on early morphogenesis and point out the usefulness of the biomechanical approach to biologists through specific examples. We will present techniques to study biomechanical phenomena from the sub-cellular to the organismal level. Finally, the application of knowledge collected through biomechanics about self-assembly and self-organization will be applied to the evolving technology of organ printing that is in vitro morphogenesis. The talk will be organized as follows:

Embryonic tissues mimic the behavior of liquids. We first overview the experimental evidence suggesting that embryonic tissues in many respect behave as fluids. One manifestation of such behavior is shown in Figure 1, which demonstrates that an initially shapeless aggregate of embryonic cells evolves to a configuration with minimal surface area (i.e. sphere), to minimize its interfacial energy, just as ordinary liquids do in the absence of external forces.

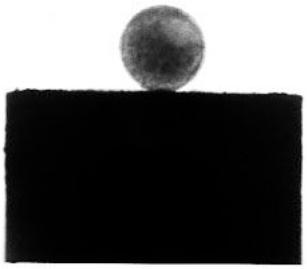

Fig. 1. The final configuration of an aggregate (~400 micron diameter) composed of appr. 40,000 chicken embryonic heart cells.

Consequences of tissue liquidity. Tissue liquidity allows the understanding of a number of early morphogentic phenomena. We will concentrate on sorting, a process in which from an initially random mixture of two (or more) cell populations one eventually nucleates and becomes surrounded by the other as shown in Figure 2. The mechanisms governing both the equilibrium shape and the kinetic approach to this state can be interpreted in terms of fluid mechanics. It will be shown how biomechanical measurements at various scales (using magnetic tweezers, AFM force manipulator, parallel plate compression device) on such systems allow to obtain valuable biologically relevant information.

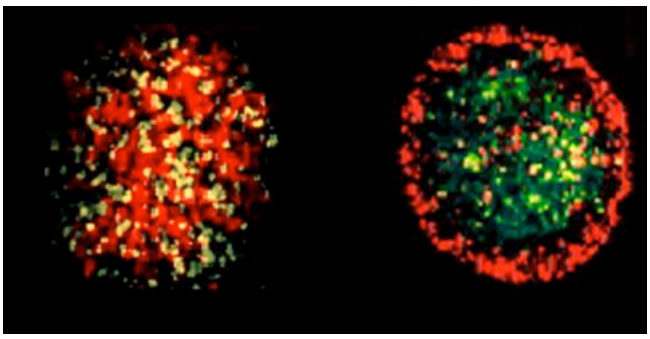

Fig. 2. Left: random initial mixture of two embryonic L cell populations transfected with N-cadherins (the green cells express 33% more cadherin than the red cells, yellow is the consequence of color mixing). Right: the final equilibrium configuration 20 hours after mixing. The linear size of the aggregates is around 200 mm.

Viscoelastic properties of extra-cellular matrices. Without the ECM the morphogenetic program cannot be fully implemented. We will overview the benefits of considering the ECM as a viscoelastic material when trying to tame morphogenetic forces.

Application to organ printing. Organ printing is an evolving technology within tissue engineering. It aims to eventually producing replacement organs in a consistent, made-to-measure manner, without the harmful consequences characterizing most of the presently used similar technologies. We will discuss this technology in some detail, but will mostly focus on how the self-organizing properties of cells and tissues, the basis of morphogenesis and their biomechanical properties, as discussed earlier, aid in the realization of this technology. In particular, we will introduce the notion of bioink and biopaper, the former being the tissue specific spherical aggregates, an example of which is shown in Figure 1 and the latter being the ECM providing the physical environment (i.e. scaffold) for printing. We will also show how computer modeling can help in optimizing this technology. An example of the evolution of a tubular organ structure, from initially printing aggregates along a circle is shown in Figure 3.

In summary, this talk is aimed at demonstrating the power of biomechanics in understanding and applying principles of morphogenesis.

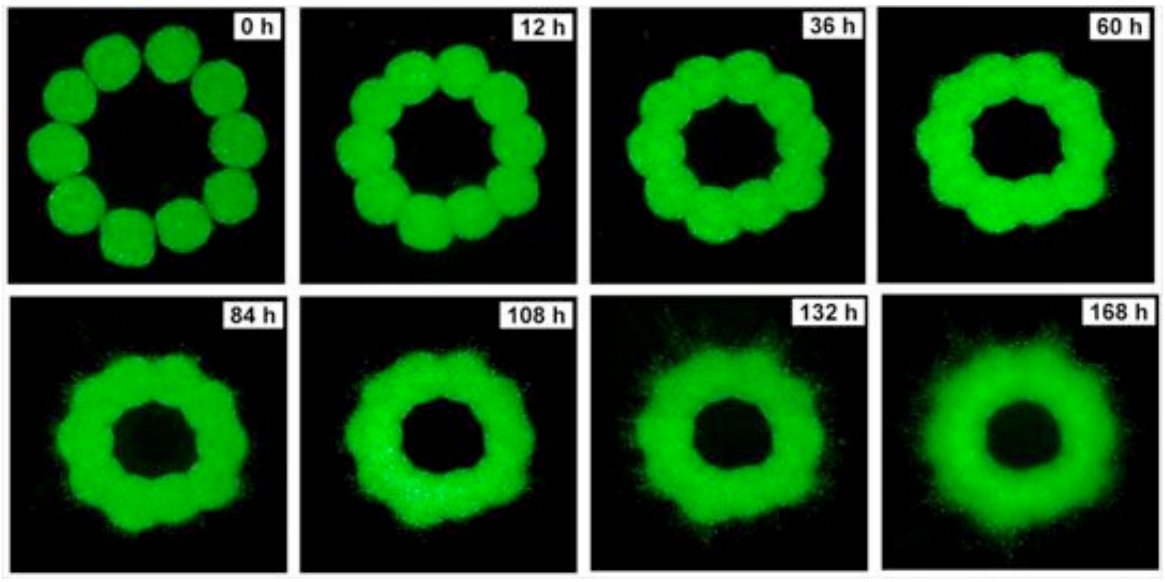

Fig. 3. Time evolution of a ring of 10 printed spherical aggregates (475 micron diameter) in a collagen gel (1.0 mg/ml concentration). Aggregates were delivered with a special bioprinter.

What we do not know about convergence and extension

Ray Keller

Studies of the cellular and molecular basis of the convergence and extension movements of the body axis in early development of vertebrates, and similar movements in other systems, have received much attention recently with the finding that components of the planar cell polarity pathway of *Drosophila* appear to regulate the polarized cell behaviors underlying convergent extension. Based on studies of cell motility in explants and manipulations of the embryo and explants, we have proposed a cell traction-cell substrate model as a guide for analyzing the cell biology and biomechanics of how this polarized cell motility might produce the mediolateral intercalation of cells that occurs during convergent extension. It seems that nearly everyone thinks that this model has a stronger underpinning in experiment than we do, and therefore I will review of the evidence for it with a focus on what is not known about cell intercalation and what should be done. I will also present evidence that suggests that an epithelial mesenchymal transition generates forces in the urodele that are generated in *Xenopus* by mediolateral intercalation, and show that urodeles share a fundamental gastrulation mechanism with amniotes.

Conserved cytomechanical modules underlying cell motility and cell rearrangements within epithelia

Ed Munro

One of the fundamental engines of metazoan morphogenesis involves the active intercalation of cells along one or more embryonic axes driving tissue convergence along those axes and (necessarily) extension along orthogonal axes. Versions of this convergent extension engine operate across the chordate phylum in a variety of different embryonic contexts and at different times during gastrulation and neurulation to shape the body axis in very different ways. And yet detailed studies of local cell behaviors underlying convergent extension in different organisms suggests a fundamentally conserved mechanism– one in which globally polarized crawling of individual cells across the surfaces of their adjacent neighbors drives progressive cell intercalation.

In the past several decades, we have learned a great deal about the cytoskeletal and adhesive machinery underlying the generation and transmission of motile forces within cells. What has become increasingly clear is that much of this machinery is highly conserved, and furthermore that it is organized into functional modules specialized e.g. for the generation of local protrusive forces; or contractile forces; or for the transmission of such forces between cells, or from cells to external substrata, via local adhesive linkages (see Figure 1).

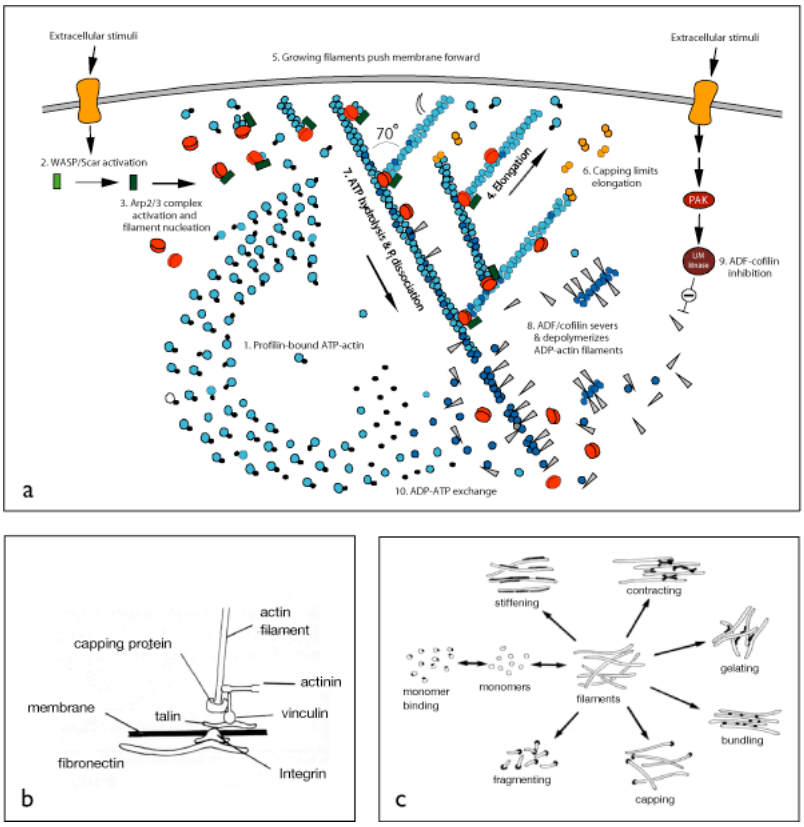

Figure 1. Cytomechanical modules underlying the crawling of animal cells across an external substratum. a) An ***Actin Polymerization Ram*** *drives localized extension at the leading edge (from Pollard et al 2000). b)* ***Integrin-based Adhesive Linkages*** *mediate the establishment of reversible contacts between cell cortex and substratum and the transmission of force through these contacts (from Bray 2000). c) A* ***Contractile Mesh*** *generates active contractile forces within the cortex that set up a tug of war between points of adhesive contact with the substratum and thereby moves the cell body forward (from Alberts et al 2003).*

Such functional modularity has important implications for how we think about specific mechanisms of convergent extension and also about the evolution of animal forms. For example, it suggests that many differences in the morphologies of related embryonic structures may arise through different tunings of the same modular machinery, through spatial or temporal differences in its deployment, or through differences in the mechanical context in which it operates.

However, it has been difficult to address these questions, or to pin down the mechanisms at work in any specific instance of convergent extension, because it has been difficult to make the conceptual leap between local force-generating processes operating at the cellular or subcellular level, and their global tissue level consequences. Physical law dictates that at any moment, local forces arising everywhere within an embryo must resolve themselves simultaneously and globally into instantaneous patterns of movement and deformation. In most cases it is beyond the human brain (or at least my brain) to intuit how they will do so.

One of our major efforts to address these issues has been to develop a computational model that can predict patterns of cell shape change and rearrangement that emerge as a consequence of local forces generated by subcellular morphogenetic modules operating within each of many cells in a close packed tissue. This model was motivated by our experimental work on epithelial cell rearrangements underlying ascidian notochord formation (Munro and Odell 2002a&b) and it builds upon the fundamental assumption, justified by our experimental observations, that embryonic cells intercalate within a close-packed monolayer by crawling across the surface of neighboring cells using the same (or functionally analogous) machinery isolated tissue culture cells use to crawl across an external substratum (Figure 2). We begin with

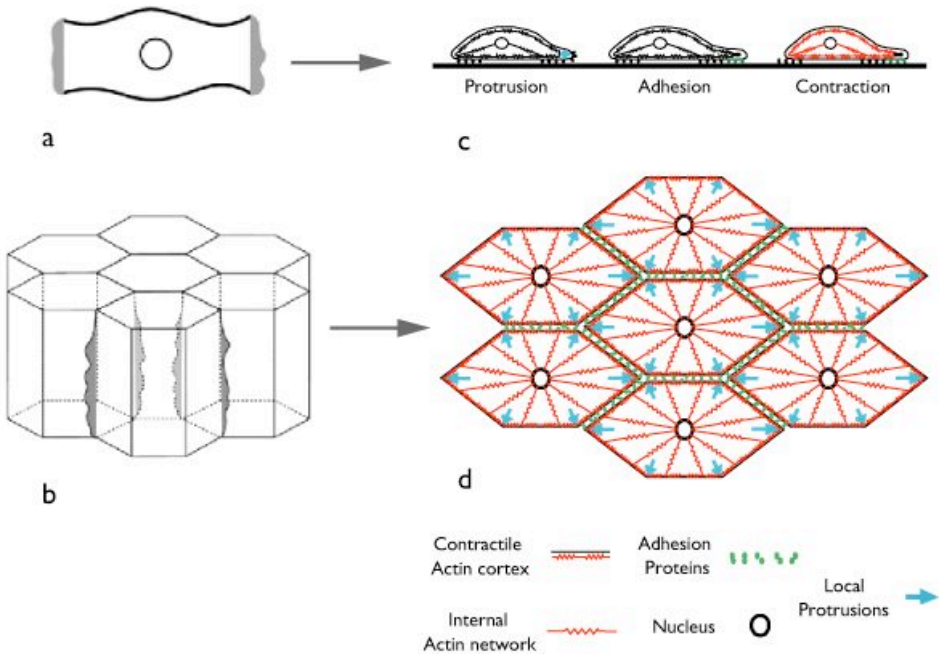

Figure 2. How the same conserved cytomechanics that propel an isolated cell across a rigid external substratum might drive convergent extension of cells within an epithelium. a & b) The basic analogy: An epithelial cell participating in convergent extension (b) crawls across the surface of its neighboring cells in the same way that an isolated cell (a) crawls across an external substratum. In particular, each internal basolateral edge of the epithelial cell is functionally analogous to a leading edge of the isolated cell. c & d) a 2D view showing how we imagine conserved (or in the case of adhesion functionally analogous) cytomechanical modules to be deployed in the isolated motile cell (c) and the epithelial cell (d) during convergent extension.

the standard textbook model for how a single cell crawls on an isolated substratum through a combination of three processes, each corresponding to one of the cytomechanical modules shown in Figure 1: 1) localized protrusive extension at the leading edge; 2) the formation of adhesive contacts with the substratum and their linkage to the cortical cytoskeleton; and 3) The generation of contractile forces within the cortex and possibly the deeper cytoplasm that sets up a tug of war between different points of adhesive contact and ultimately moves the cell forward. We build a single model cell from a collection of discrete interconnected mechanical elements, each of which represents a piece of the cortex or internal cytoplasm or an adhesive linkage; and we endow these elements with mechanical and kinetic properties designed to mimic, as closely as possible, those of their real counterparts. We do so in a way that allows us to map experimental measurements of cytoskeletal or adhesive mechanics onto the parameters that govern each element's behaviors.

We have been using this model in a number of different ways. One is to ask whether the same machinery that endows a single cell with the ability to crawl across an isolated substratum could also account qualitatively and quantitatively for the ability of a sheet of close-packed cells to converge and extend (it can). Another is to ask whether the ability to converge and extend is robust with respect to variations in the parameters that govern the behaviors of model elements (it is, suggesting that the real convergent extension engine may be similarly robust to genetic variation in the underlying morphogenetic machinery). More generally, we can ask how patterns of cell shape change and rearrangement depend either on the local cytoskeleletal and adhesive mechanics operating within each cell, or upon global physical constraints arising through contacts with adjacent tissues.

References:

Munro EM, Odell GM (2002a) Polarized basolateral cell motility underlies invagination and convergent extension of the ascidian notochord. Development 129:13-24

Munro EM, Odell GM (2002b) Morphogenetic pattern formation during ascidian notochord formation is regulative and highly robust. Development 129:1-12